



# Modeling Rabies Transmission in Spatially Heterogeneous Environments via $\theta$ -diffusion

Xiunan Wang<sup>1</sup>  · Hao Wang<sup>1</sup> · Michael Y. Li<sup>1</sup>

Received: 3 September 2020 / Accepted: 31 December 2020 / Published online: 12 January 2021  
© The Author(s), under exclusive licence to Society for Mathematical Biology 2021

## Abstract

Rabies among dogs remains a considerable risk to humans and constitutes a serious public health concern in many parts of the world. Conventional mathematical models for rabies typically assume homogeneous environments, with a standard diffusion term for the population of rabid animals. It has recently been recognized, however, that spatial heterogeneity plays an important role in determining spatial patterns of rabies and the cost-effectiveness of vaccinations. In this paper, we develop a spatially heterogeneous dog rabies model by using the  $\theta$ -diffusion equation, where  $\theta$  reflects the way individual dogs make movement decisions in the underlying random walk. We numerically investigate the dynamics of the model in three diffusion cases: homogeneous, city-wild, and Gaussian-type. We find that the initial conditions affect whether traveling waves or epizootic waves can be observed. However, different initial conditions have little impact on steady-state solutions. An “active” interface is observed between city and wild regions, with a “ridge” on the city side and a “valley” on the wild side for the infectious dog population. In addition, the progressing speed of epizootic waves changes in heterogeneous environments. It is impossible to eliminate rabies in the entire spatial domain if vaccination is focused only in the city region or only in the

---

Research of XW is partially supported by IUSEP Funding and HW’s NSERC Discovery Grant. Research of HW is partially supported by the Natural Science and Engineering Research Council of Canada (NSERC) through Discovery Grant RGPIN-2020-03911 and Accelerator Grant RGPAS-2020-00090. Research of MYL is partially supported by the Natural Science and Engineering Research Council of Canada (NSERC) Grant RGPIN 05395 Li.

---

✉ Xiunan Wang  
xiunan@ualberta.ca

Hao Wang  
hao8@ualberta.ca

Michael Y. Li  
myli@ualberta.ca

<sup>1</sup> Department of Mathematical and Statistical Sciences, University of Alberta, Edmonton AB T6G 2G1, Canada

wild region. When a seasonal transmission is incorporated, the dog population size approaches a positive time-periodic spatially heterogeneous state eventually.

**Keywords** Rabies · Diffusion · Fokker–Planck equation · Traveling wave · Vaccination · Spatial heterogeneity

## 1 Introduction

Rabies is a zoonotic viral disease which brings serious public health and economic concerns, causing about 59,000 human deaths annually and an estimated cost of US\$ 8.6 billion globally per year (World Health Organization 2020). It also threatens the persistence of some endangered wildlife species (Stuchin et al. 2018). Rabies virus is normally transmitted via the bites of infected animals whose saliva contain the virus. The infection is invariably fatal once the virus arrives at the central nervous system. If the virus reaches the limbic system, then the infected animals become aggressive, lose their sense of direction, and wander around almost randomly (Kaplan 1977; Macdonald 1980). The duration between the initial infection and the appearance of symptoms varies among species and also depends on the location of the wounds as well as how many viruses are injected in, but infected animals typically die in one week after symptoms appear. Although all mammals can be infected with rabies, only a few species, such as dogs, cats, foxes, bats, raccoons, skunks, coyotes and mongooses, are important reservoirs for the disease (Center for Disease Control and Prevention 2019). In particular, dogs act as a primary transmitter of rabies to humans, accounting for 99% of all human rabies deaths worldwide (World Health Organization 2020). With a fast population growth of domestic dogs, the risk of humans getting rabies keeps increasing. Vaccinating dogs has been recommended as the most cost-effective control strategy of rabies in humans. It can help reduce human rabies deaths and the need for post-exposure prophylaxis (World Health Organization 2020).

Understanding the spatial and temporal dynamics of rabies transmission is crucial for predicting and controlling rabies epidemics. Mathematical modeling via partial differential equations have made significant contributions to gaining insights into spatial patterns of rabies transmission. Meanwhile, observed epidemic waves of rabies in history together with the phenomenon of random movement of rabid animals due to clinical symptoms provide an appropriate system for mathematicians to explore spatial and temporal dynamics of infectious diseases by developing reaction–diffusion equation models, analyzing the existence of traveling waves, calculating the minimum spreading speed, and explaining data.

Epidemiological modeling of rabies dates back to the 1980s. Anderson et al. (1981) used an ordinary differential equation model, with susceptible, infected yet not infectious and infectious compartments, to explain the observed 3 to 5 year population cycle in foxes infected with rabies in Europe and discussed the effects of culling and vaccinating foxes in the control of rabies. To study the westward epizootic waves of rabies in foxes crossing the continental Europe after World War II, Källén et al. (1985) and Murray et al. (1986) extended the model in Anderson et al. (1981) to include the diffusion of rabid foxes. They calculated the minimum speed of the traveling wave

front, determined the threshold for the occurrence of an epizootic, and suggested the required width of a barrier in which the susceptible fox population is adequately diminished to prevent the rabies wave front from progressing to a disease-free area. Ou and Wu (2006) revisited the spatial spread of rabies in Europe between 1945 and 1985 by developing a stage-structured delay reaction–diffusion equation model and considered the distinction of the territorial behavior between juvenile and adult foxes and they showed that the minimum wave speed is a decreasing function of the maturation duration. Borchering et al. (2012) constructed a reaction–diffusion model to study the interspecies transmission of rabies in bat and skunk populations, and their simulations indicated that a model with a reservoir of overlapping species is better than a single species rabies model at reproducing the spatial spread of rabies in Texas. In recent years, there has been an increasing number of research works on modeling rabies in dog populations. Zhang et al. (2012) formulated a reaction–diffusion equation model to study rabies transmission in dog populations and the transmission of rabies from dogs to humans. They derived the minimum wave speed and numerically showed the existence of traveling waves. We refer to the reviews by Panjeti and Real (2011), Ruan (2017a), Ruan (2017b) and Sterner and Smith (2006) for more references on various rabies models.

Most of the existing reaction–diffusion rabies models adopt a constant diffusion rate of the rabid animals under the assumption of spatially homogeneous environments, which certainly renders much tractability for mathematical analysis. However, spatial heterogeneity can play an important role in affecting the magnitude and spread of rabies among animals considering that rabies are usually transmitted over a large geographical region. For example, large rivers have been found to lead to a seven-fold reduction in the local propagation rates (Smith et al. 2002) and high elevation peaks in mountains can markedly constrain rabies expansions (Benavides et al. 2016). In addition, vaccination has been demonstrated to be less effective in controlling raccoon rabies in homogeneous good-quality habitat and highly spatially heterogeneous bad-quality habitat than in good-quality habitat with high spatial heterogeneity (Rees et al. 2013). Some stochastic and agent-based rabies models have incorporated spatial heterogeneity (see, e.g., Allen et al. 2002; Mollison and Kuulasmaa 1985; Voigt and MacDonald 1984); however, reaction–diffusion rabies models that consider spatial heterogeneity are rare (see, e.g., Neilan and Lenhart 2011). Neilan and Lenhart (2011) formulated an SIR reaction–diffusion–advection model to characterize an optimal vaccination control of rabies among raccoons. Their numerical results revealed that natural land features and the relocation of raccoons can considerably affect the design of a cost-effective vaccination program. When landscape spatial heterogeneity is involved, the diffusion rate is no longer constant and different diffusion laws can lead to different outcomes. For instance, however successful Fick’s law has been in describing the diffusion of microspecies or microparticles, there are situations where Fick’s law may not be appropriate for animal movements. Fickian diffusion equation tends to equalize population in different locations of the habitat. In contrast, Fokker–Planck equation, which was originally derived in order to study Brownian motion, allows accumulation of population in locations where mobility is lower. For this reason, a number of researchers have suggested that Fokker–Planck equation should be a better model for

describing animal movements in spatially heterogeneous environments (Potapov et al. 2014; Turchin 1998).

Recently, Potapov et al. (2014) derived a  $\theta$ -diffusion equation from a random walk with transition probabilities depending on decision point, reflected by a parameter  $\theta$ , on a uniform one-dimensional grid space. The parameter  $\theta$  can take any value between 0 and 1. When the diffusion rate is spatially heterogeneous, different values of  $\theta$  give rise to different equations. Making decisions at the departure point (when  $\theta = 0$ ), the midpoint (when  $\theta = 0.5$ ) and the destination point (when  $\theta = 1$ ) of a single step movement correspond to Fokker–Planck equation, Fickian diffusion equation, and the attractive dispersal equation, respectively. By using an optimization technique, Potapov et al. showed that the Fokker–Planck dispersal (i.e., repulsive dispersal) and the attractive dispersal are evolutionarily stable strategies. The purpose of this paper is to use the  $\theta$ -diffusion equation in Potapov et al. (2014) to formulate a dog rabies model which incorporates spatially varying diffusivity and to investigate rabies transmission dynamics and control effects under different circumstances.

The rest of the paper is organized as follows. In the next section, we formulate our dog rabies model with  $\theta$ -diffusion. In Sect. 3, we derive the basic reproduction number associated with the ODE system. In Sects. 4, 5, and 6, we numerically explore dynamics of the model with homogeneous, city-wild and Gaussian-type diffusions, respectively. In Sect. 7, we present some preliminary result for an improved rabies model with seasonality. We end this paper by a discussion in Sect. 8.

## 2 Model Formulation

Starting from a random walk model, Potapov et al. (2014) derived the following  $\theta$ -diffusion equation

$$\frac{\partial u(x, t)}{\partial t} = \frac{\partial}{\partial x} \left( D^{2\theta}(x) \frac{\partial}{\partial x} (D^{1-2\theta}(x) u(x, t)) \right),$$

where  $u(x, t)$  represents the population of an animal species at location  $x$  and time  $t$ ,  $D(x)$  is the diffusion rate at location  $x$ , and  $\theta \in [0, 1]$  reflects the way individuals make movement decisions in the underlying random walk. When  $D(x)$  is constant, different values of  $\theta$  result in the same equation  $u_t = Du_{xx}$  and hence different decision makings give the same outcome. When  $D(x)$  is spatially dependent, the derived  $\theta$ -diffusion equation is a family of infinitely many partial differential equations. Among them are three special ones: Fokker–Planck equation  $u_t = (Du)_{xx}$  (when  $\theta = 0$ ), Fickian diffusion equation  $u_t = (Du_x)_x$  (when  $\theta = 0.5$ ), and the attractive dispersal equation  $u_t = (D^2(u/D)_x)_x$  (when  $\theta = 1$ ). Fokker–Planck equation arises from a repulsive transition where individuals tend to leave areas of low fitness and the transition probability depends on the condition at the departure point (Okubo and Levin 2001). In this case, individuals have the same probability of moving left and right and hence Fokker–Planck equation can be used to describe the diffusion of individuals who move randomly. Fickian diffusion equation results from a neutral transition and the transition probability depends on the local fitness at the midpoint

between the departure point and the destination point. In this case, individuals have the same probability of moving between two locations and hence Fickian diffusion equation is applicable to symmetric movement. The attractive dispersal equation is derived from an attractive transition where individuals are attracted to move toward areas of high fitness and the transition probability depends on the state at the destination point.

Recently, Zhang et al. (2012) developed a reaction–diffusion equation model with standard diffusion terms to investigate rabies transmission among dog and human populations. In their model, the equations for human compartments are decoupled from the equations for dog compartments since rabies cannot be transmitted from humans to dogs, and the subsystem for the dog population is given by system (1). The dog population is classified into four compartments: susceptible, exposed, infectious, and vaccinated, and the number of dogs in each compartment at location  $x$  and time  $t$  is  $S(x, t)$ ,  $E(x, t)$ ,  $I(x, t)$ , and  $R(x, t)$ , respectively. The dog-to-dog biting rate is  $\beta$ . If a susceptible dog is bitten by an infectious dog, then it will enter the exposed compartment and it may or may not develop clinical outcomes. The incubation period of rabies in dogs is  $1/\sigma$ , and the risk factor of clinical outcome of exposed dogs is  $\gamma$ . Hence,  $\sigma\gamma E(x, t)$  gives the number of exposed dogs that develop clinical rabies per year at location  $x$  and  $\sigma(1 - \gamma)E(x, t)$  represents those that do not develop clinical outcomes and return to the susceptible compartment. Susceptible and exposed dogs are vaccinated at the same rate  $k$  and the vaccination immunity is lost at a rate  $\lambda$ . The recruitment rate of dogs is  $a$ . The natural death rate is  $m$ , and the disease-induced death rate is  $\mu$ . The diffusion rates of dogs in the four compartments are  $D_S$ ,  $D_E$ ,  $D_I$ , and  $D_R$ , respectively, which measure how far an individual dog travels on average from its original location per year (Fofana and Hurford 2017).

$$\begin{aligned} \frac{\partial S(x, t)}{\partial t} &= a + \lambda R(x, t) + \sigma(1 - \gamma)E(x, t) - \beta S(x, t)I(x, t) \\ &\quad - (m + k)S(x, t) + D_S \frac{\partial^2 S(x, t)}{\partial x^2}, \\ \frac{\partial E(x, t)}{\partial t} &= \beta S(x, t)I(x, t) - \sigma E(x, t) - (m + k)E(x, t) + D_E \frac{\partial^2 E(x, t)}{\partial x^2}, \quad (1) \\ \frac{\partial I(x, t)}{\partial t} &= \sigma\gamma E(x, t) - (m + \mu)I(x, t) + D_I \frac{\partial^2 I(x, t)}{\partial x^2}, \\ \frac{\partial R(x, t)}{\partial t} &= k(S(x, t) + E(x, t)) - (m + \lambda)R(x, t) + D_R \frac{\partial^2 R(x, t)}{\partial x^2}, \end{aligned}$$

for  $t > 0$ ,  $x \in \Omega$ , with homogeneous Neumann boundary condition

$$\frac{\partial S}{\partial x} = \frac{\partial E}{\partial x} = \frac{\partial I}{\partial x} = \frac{\partial R}{\partial x} = 0 \quad \text{at } x \in \partial\Omega.$$

They discussed the local stability of the endemic equilibrium, derived the minimal wave speed analytically, and investigated the existence of traveling waves and the influences of parameters on the minimal wave speed by numerical simulations. Their

analysis shows that dog movement can lead to traveling waves and greatly influences the minimal wave speed, which implies that restricting the movement of exposed and infectious dogs may be an effective measure to prevent rabies transmission.

Next, we will develop our rabies model based on model (1) by applying the  $\theta$ -diffusion equation. We clarify the following assumptions:

- (i) Considering that infectious dogs have impaired central nervous systems and hence are lack of sense of direction (Center for Disease Control and Prevention 2019), we assume that all infectious dogs move randomly and non-infectious dogs can make any movement decisions.
- (ii) The recruitment of new susceptible dogs may result from both new borns and the importation of dogs into a region from outside regions for commercial transaction, and the recruitment rate is assumed to be a constant  $a$ .
- (iii) Susceptible and exposed dogs are vaccinated at the same rate  $k$ . In some less developed countries, people may not be able to afford the vaccination or are not willing to vaccinate their healthy dogs and may only vaccinate the dogs when they find that their dogs are bitten by other rabid animals. In that case, the vaccination rate of exposed dogs may be higher than that of susceptible dogs in a local region. However, in some countries, most susceptible dogs are vaccinated. Then the effective vaccination rate of susceptible dogs should be higher than that of exposed dogs. Here we consider a case that lies between these two cases and assume that the vaccination rates of susceptible and exposed dogs are the same.
- (iv) If a susceptible dog is bitten by an infectious dog, then it will enter the exposed compartment and the risk factor for it to develop clinical rabies is  $\gamma$ .

According to assumption (i), we can use the Fokker–Planck dispersal term, obtained by letting  $\theta = 0$  in the  $\theta$ -diffusion equation, to describe the diffusion of the population of infectious dogs. In contrast, susceptible, exposed, and vaccinated dogs can make movement decisions depending on the state at the starting point ( $\theta = 0$ ), the ending point ( $\theta = 1$ ) or some point between the starting and ending points ( $\theta \in (0, 1)$ ) of the movement at each single step. In more complex cases, a non-infectious dog may adopt a comprehensive strategy by having a range of different values of  $\theta$  in making movement decisions. For simplicity, if we assume that all susceptible, exposed, and vaccinated dogs use the same strategy in movement (i.e., the same value of  $\theta$  for the diffusion terms of these three compartments), then we have the following model:

$$\begin{aligned} \frac{\partial S(x, t)}{\partial t} &= a + \lambda R(x, t) + \sigma(1 - \gamma)E(x, t) - \beta S(x, t)I(x, t) - (m + k)S(x, t) \\ &\quad + \frac{\partial}{\partial x} \left( D_S^{2\theta}(x) \frac{\partial}{\partial x} (D_S^{1-2\theta}(x) S(x, t)) \right), \\ \frac{\partial E(x, t)}{\partial t} &= \beta S(x, t)I(x, t) - \sigma E(x, t) - (m + k)E(x, t) \\ &\quad + \frac{\partial}{\partial x} \left( D_E^{2\theta}(x) \frac{\partial}{\partial x} (D_E^{1-2\theta}(x) E(x, t)) \right), \\ \frac{\partial I(x, t)}{\partial t} &= \sigma \gamma E(x, t) - (m + \mu)I(x, t) + \frac{\partial^2}{\partial x^2} (D_I(x) I(x, t)), \end{aligned}$$

**Table 1** Biological interpretations and values for parameters of model (2)

Parameter	Description	Value	Unit	Source
$a$	Recruitment rate	100	#dogs year <sup>-1</sup>	Assumption
$\lambda$	Loss rate of immunity	1	year <sup>-1</sup>	Zinsstag et al. (2009)
$1/\sigma$	Incubation period	1/6	year	Center for Disease Control and Prevention 2019
$\gamma$	Risk factor for clinical outcome	0.4		Zhang et al. (2012), Zinsstag et al. (2009)
$\beta$	Dog-to-dog biting rate	0.25	dog <sup>-1</sup> year <sup>-1</sup>	Estimated
$m$	Natural mortality rate	0.08	year <sup>-1</sup>	Zhang et al. (2012)
$k$	Vaccination rate	[0, 1]	year <sup>-1</sup>	
$\mu$	Disease-induced death rate	64.04	year <sup>-1</sup>	Hampson et al. (2007)
$\theta$	Fractional order for a dog's decision	[0, 1]		Potapov et al. (2014)
$D_S(x)$	Diffusion rate of susceptible dogs	Varied	km <sup>2</sup> year <sup>-1</sup>	
$D_E(x)$	Diffusion rate of exposed dogs	Varied	km <sup>2</sup> year <sup>-1</sup>	
$D_I(x)$	Diffusion rate of infectious dogs	Varied	km <sup>2</sup> year <sup>-1</sup>	
$D_R(x)$	Diffusion rate of vaccinated dogs	Varied	km <sup>2</sup> year <sup>-1</sup>	

$$\frac{\partial R(x, t)}{\partial t} = k(S(x, t) + E(x, t)) - (m + \lambda)R(x, t) + \frac{\partial}{\partial x} \left( D_R^{2\theta}(x) \frac{\partial}{\partial x} (D_R^{1-2\theta}(x) R(x, t)) \right), \tag{2}$$

for  $t > 0, x \in \Omega$ , with homogeneous Neumann boundary condition

$$\frac{\partial S}{\partial x} = \frac{\partial E}{\partial x} = \frac{\partial I}{\partial x} = \frac{\partial R}{\partial x} = 0 \text{ at } x \in \partial\Omega.$$

In Table 1, we list the biological interpretations and the estimated values of the parameters.

In reality, all the parameters in model (2) can be spatially dependent. For example, the recruitment rate and the biting rate may be different in different landscapes. The vaccination rate can also be spatially heterogeneous since vaccines are usually distributed by helicopters or aircrafts and dogs living along or near the helicopter or aircraft distribution routes are easier to develop immunity to rabies via biting into or swallowing the vaccine baits compared with those living far away from the routes. In order to focus on investigating the role of the diffusion of rabid dogs in the disease

transmission, we consider the following model in which only the diffusion rate of infectious dogs are spatially dependent whereas the diffusion rates of non-infectious dogs as well as the other parameters are constant. This is also reasonable considering that the movements of non-infectious dogs are typically territorial and the diffusion rate of infectious dogs is significantly larger.

$$\begin{aligned}
 \frac{\partial S(x, t)}{\partial t} &= a + \lambda R(x, t) + \sigma(1 - \gamma)E(x, t) - \beta S(x, t)I(x, t) - (m + k)S(x, t), \\
 \frac{\partial E(x, t)}{\partial t} &= \beta S(x, t)I(x, t) - \sigma E(x, t) - (m + k)E(x, t), \\
 \frac{\partial I(x, t)}{\partial t} &= \sigma \gamma E(x, t) - (m + \mu)I(x, t) + \frac{\partial^2}{\partial x^2}(D_I(x)I(x, t)), \\
 \frac{\partial R(x, t)}{\partial t} &= k(S(x, t) + E(x, t)) - (m + \lambda)R(x, t),
 \end{aligned} \tag{3}$$

for  $t > 0$ ,  $x \in \Omega$ , with homogeneous Neumann boundary condition

$$\frac{\partial S}{\partial x} = \frac{\partial E}{\partial x} = \frac{\partial I}{\partial x} = \frac{\partial R}{\partial x} = 0 \quad \text{at } x \in \partial\Omega.$$

In all the numerical simulations of this paper, we set  $\Omega = [0, 100]$ . This one-dimensional spatial domain can be regarded as an abstract projection of the two-dimensional space.

### 3 Basic Reproduction Number

In this section, we use the next generation matrix method (see Diekmann et al. 1990; van den Driessche and Watmough 2002) to derive the basic reproduction number for the associated ODE system

$$\begin{aligned}
 \frac{dS(t)}{dt} &= a + \lambda R(t) + \sigma(1 - \gamma)E(t) - \beta S(t)I(t) - (m + k)S(t), \\
 \frac{dE(t)}{dt} &= \beta S(t)I(t) - \sigma E(t) - (m + k)E(t), \\
 \frac{dI(t)}{dt} &= \sigma \gamma E(t) - (m + \mu)I(t), \\
 \frac{dR(t)}{dt} &= k(S(t) + E(t)) - (m + \lambda)R(t).
 \end{aligned} \tag{4}$$

In mathematical epidemiology, basic reproduction number is the expected number of secondary infections produced, in a totally susceptible population, by a typical infectious individual. It characterizes the threshold for an emerging disease to persist or to be eliminated. System (4) has a disease-free equilibrium  $(S^0, 0, 0, R^0)$  where

$$S^0 = \frac{a(m + \lambda)}{m(m + \lambda + k)}, \quad R^0 = \frac{ka}{m(m + \lambda + k)}.$$

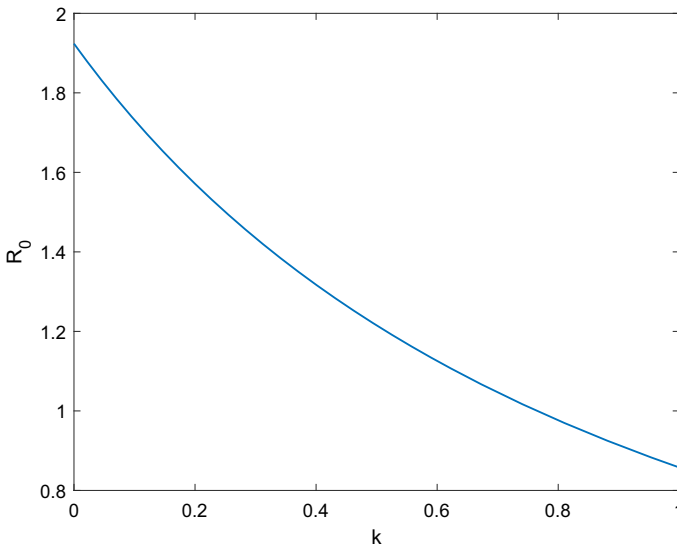


**Fig. 1**  $R_0$  as a function of  $k$ . The other parameter values are the same as those in Table 1

Linearizing system (4) at  $(S^0, 0, 0, R^0)$  we get the following system for the  $E$  and  $I$  compartments:

$$\begin{aligned} \frac{\partial E(t)}{\partial t} &= \beta S^0 I(t) - \sigma E(t) - (m + k)E(t), \\ \frac{\partial I(t)}{\partial t} &= \sigma \gamma E(t) - (m + \mu)I(t). \end{aligned} \tag{5}$$

Rewrite system (5) as

$$\frac{du}{dt} = (F - V)u$$

where

$$F = \begin{bmatrix} 0 & \beta S^0 \\ 0 & 0 \end{bmatrix}$$

and

$$V = \begin{bmatrix} \sigma + m + k & 0 \\ -\sigma \gamma & m + \mu \end{bmatrix}.$$

Then we have the basic reproduction number  $\mathcal{R}_0 := r(FV^{-1})$ , the spectral radius of  $FV^{-1}$ .

Figure 1 shows that  $R_0$  is a decreasing function of the vaccination rate  $k$  and it indicates that a vaccination rate greater than 0.76 can decrease  $R_0$  to be less than 1.

Recently, there have been some works (see, e.g., Liang et al. 2017; Magal et al. 2019; Wang and Zhao 2012) on basic reproduction number for PDE systems with standard diffusion (i.e., Fickian diffusion) such as  $Du_{xx}$ , where  $D$  is a constant diffusion rate, or  $(D(x)u_x)_x$ , where  $D(x)$  is a spatial dependent diffusion rate. However, it remains challenging and interesting to derive the basic reproduction number for PDE systems with non-standard diffusion terms such as Fokker–Planck diffusion [e.g., system (3)] or attractive dispersal diffusion.

## 4 Homogeneous Diffusion

In this section, we investigate dynamics of system (3) for the simplest case of homogeneous diffusion which can be used as a benchmark and may facilitate us to identify the factor determining whether traveling waves can be observed. We consider two types of initial conditions: homogeneous and stepwise. The homogeneous initial condition represents an initial state in which the infected dogs are uniformly distributed in space (see Sect. 4.1.1). With the stepwise initial condition, the infected dogs are assumed to be equally distributed over a subinterval of the entire spatial domain at the starting time point (see Sect. 4.1.2). We discretize the spatial domain  $[0, 100]$  by stepsize 1, and then with the homogeneous initial condition in Sect. 4.1.1 there are  $(800 + 5 + 1 + 10) \times 101 = 82,416$  dogs.

### 4.1 Initial Conditions

#### 4.1.1 Homogeneous Initial Condition

$$S(x, 0) = 800, E(x, 0) = 5, I(x, 0) = 1, R(x, 0) = 10.$$

#### 4.1.2 Stepwise Initial Condition

If  $x \in [0, 25]$ ,

$$S(x, 0) = S^*, E(x, 0) = E^*, I(x, 0) = I^*, R(x, 0) = R^*.$$

If  $x \in (25, 100]$ ,

$$S(x, 0) = S^0, E(x, 0) = 0, I(x, 0) = 0, R(x, 0) = R^0.$$

Here  $(S^*, E^*, I^*, R^*)$  is the unique endemic equilibrium of system (4) where

$$S^* = \frac{(m + \sigma + k)(m + \mu)}{\beta\sigma\gamma}, E^* = \frac{(m + \mu)I^*}{\sigma\gamma},$$

$$I^* = \frac{m(m + \lambda + k)[\beta S^0\sigma\gamma - (m + k + \sigma)(m + \mu)]}{\beta(m + \mu)[m(m + \lambda + k) + \sigma\gamma(m + \lambda)]}, R^* = \frac{k(S^* + E^*)}{m + \lambda}.$$

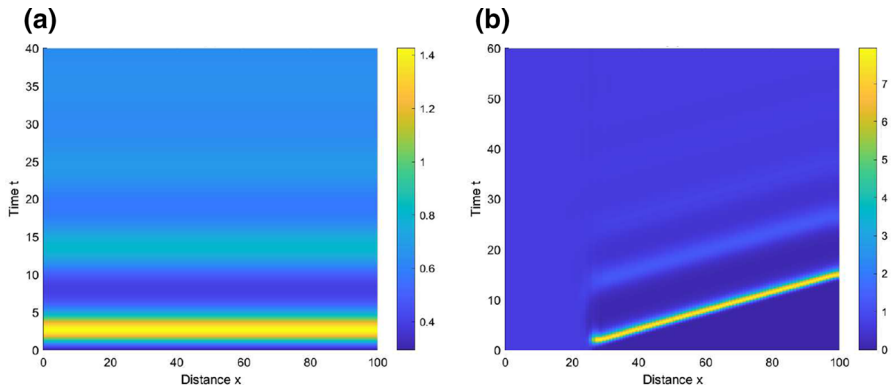


**Fig. 2** **a** The 2-D view of long-term spatial distribution of infectious dogs with homogeneous initial condition given in Sect. 4.1.1; **b** The 2-D view of long-term spatial distribution of infectious dogs with stepwise initial condition given in Sect. 4.1.2.  $D_I(x) = 5$ ,  $k = 0.09$ , and the other parameter values are the same as those in Table 1

## 4.2 Long-Term Dynamics and Traveling Waves

Figure 2 shows the long-term spatial distribution of infectious dogs under the homogeneous initial condition (given in Sect. 4.1.1) and the stepwise initial condition (given in Sect. 4.1.2). The long-term spatial distributions of dogs in all the four compartments under these two different initial conditions are given in supplementary Figs. 17 and 18, respectively (see Appendix). Figure 3 gives the distributions of susceptible, exposed, infectious, and vaccinated dogs at the end of every other year under the stepwise initial condition. From these figures, we see that in the case of homogeneous diffusion, traveling waves or epizootic waves can be observed with stepwise initial condition but not with homogeneous initial condition. However, different initial conditions have little impact on the steady states. When traveling waves or epizootic waves are observed, the waves travel to disease-free areas as time passes. With either the homogeneous initial condition or the stepwise initial condition, the first outbreak is followed by a second outbreak with much smaller peaks.

## 5 City-Wild Diffusion

In this section, we study the dynamics of system (3) with diffusion in city-wild landscape. City-wild diffusion provides us with an ideal case to study the spatial transmission and control of rabies in heterogeneous environments. Dogs have smaller diffusion rates in the city region than in the wild since the city region contains a lot of buildings, houses, traffics, and human activities, whereas the wild region is an open field unoccupied by humans and hence less impedes the movement of dogs. Since some dogs can wander back and forth between city and wild regions, rabies in the city region may be transmitted to the wild region bringing a risk to wildlife. Meanwhile, rabies in the wild region may also spread to the city region posing a threat to public health.

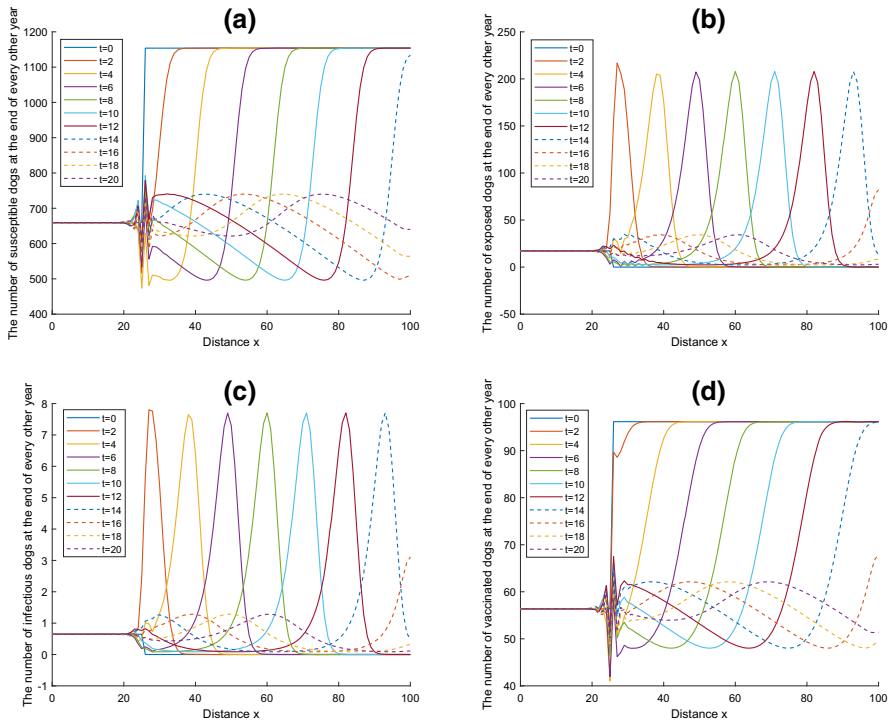


**Fig. 3** The number of susceptible, exposed, infectious, and vaccinated dogs at the end of every other year with the stepwise initial condition given in Sect. 4.1.2.  $D_I(x) = 5$ ,  $k = 0.09$ , and the other parameter values are the same as those in Table 1

We divide the spatial domain  $[0, 100]$  into two subintervals letting  $[0, 50]$  represent the city region and  $(50, 100]$  the wild region. We suppose that the average diffusion rate of infectious dogs is about 500 meters per year in the city region and 7 kilometers per year in the wild region. We also assume that the diffusion rate in the interface between city and wild regions increases strictly and smoothly. In order to fit this certain qualitative shape, we try transformations for the arctan function and choose to use the function  $D_I(x) = \frac{13}{6} \arctan(x - 50) + \frac{15}{4}$  to describe the city-wild diffusion rate of infectious dogs (see Fig. 4).

### 5.1 Initial Conditions

We consider the homogeneous initial condition (i.e., uniform distribution of infectious dogs) and heterogeneous initial conditions with local infections in the city region, in the wild region and around the city-wild interface, respectively. We would like to see how these different initial conditions together with the city-wild landscape impact rabies transmission dynamics as well as the effects of control measures.

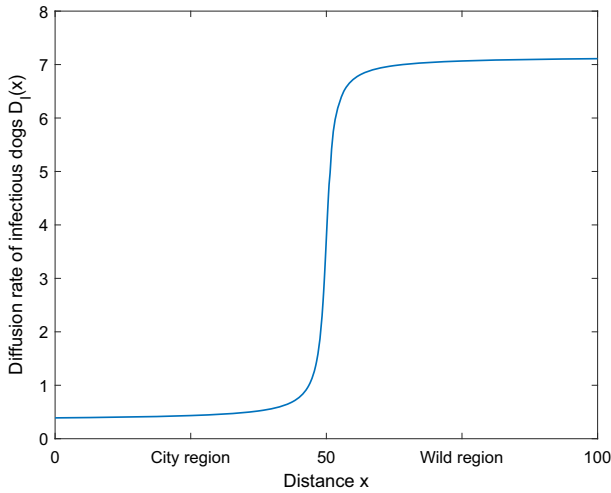


Fig. 4 City-wild diffusion rate of infectious dogs.  $D_I(x) = \frac{13}{6} \arctan(x - 50) + \frac{15}{4}$

### 5.1.1 Homogeneous Initial Condition

$$S(x, 0) = 800, E(x, 0) = 5, I(x, 0) = 1, R(x, 0) = 10.$$

### 5.1.2 Initial Condition with Infections in City Region

If  $x \in [0, 25]$ ,

$$S(x, 0) = S^*, E(x, 0) = E^*, I(x, 0) = I^*, R(x, 0) = R^*.$$

If  $x \in (25, 100]$ ,

$$S(x, 0) = S^0, E(x, 0) = 0, I(x, 0) = 0, R(x, 0) = R^0.$$

### 5.1.3 Initial Condition with Infections in Wild Region

If  $x \in [0, 75)$ ,

$$S(x, 0) = S^0, E(x, 0) = 0, I(x, 0) = 0, R(x, 0) = R^0.$$

If  $x \in [75, 100]$ ,

$$S(x, 0) = S^*, E(x, 0) = E^*, I(x, 0) = I^*, R(x, 0) = R^*.$$

#### 5.1.4 Initial Condition with Infections Around the Interface Between City and Wild Regions

If  $x \in [0, 40) \cup (60, 100]$ ,

$$S(x, 0) = S^0, E(x, 0) = 0, I(x, 0) = 0, R(x, 0) = R^0.$$

If  $x \in [40, 60]$ ,

$$S(x, 0) = S^*, E(x, 0) = E^*, I(x, 0) = I^*, R(x, 0) = R^*.$$

### 5.2 Long-Term Dynamics and Epizootic Waves

The long-term spatial distributions of dogs under the above four different initial conditions are given in supplementary Figs. 19, 20, 21 and 22, respectively. In order to have a closer look at how the epizootics progress temporally and spatially, we plot the distribution of dogs in each compartment at the end of every ten years in Fig. 5 for the homogeneous initial condition, and at the end of every other year in Figs. 6, 7 and 8 for the three heterogeneous initial conditions. There is little difference between the steady states in these figures, which indicates that the initial conditions have little impact on the long-term spatial distribution of dogs in the city-wild diffusion case.

Compared with the homogeneous diffusion case in Sect. 4, a major difference that arises in the city-wild diffusion is the “active” interface between city and wild regions. Flows of susceptible and vaccinated dogs from the city region can enter the wild region and flows of exposed and infectious dogs from the wild region can enter the city region. Note that the only difference between the homogeneous diffusion case and the city-wild diffusion case under the same initial condition is the diffusion rate of infectious dogs. Thus, it is the city-wild diffusion rate of infectious dogs that results in the “ups and downs” around the interface between city and wild regions. A possible explanation for this phenomenon near the interface is that the frequency or probability of dogs moving from the wild region to the city region is higher than that of moving from the city region to the wild region since the diffusion rate in the wild region is higher. Once infectious dogs in the wild region enter into the city region their diffusion rate decreases since their movement becomes hindered by the more obstacles in the city region, which makes them easy to accumulate on the city side of the interface. Meanwhile, the population of infectious dogs at the wild locations near the interface drop below the average level of population in the inner wild region. More infectious dogs staying on the city side near the interface leads to more susceptible dogs becoming infected there. Then, the number of susceptible dogs decreases and the number of exposed dogs increases on the city side near the interface. Since these exposed dogs will become infectious soon, in turn there will be more infectious dogs soon on the city side. Similarly, fewer infectious dogs staying on the wild side near the interface results in fewer susceptible dogs becoming infected, and hence, there are more susceptible dogs and fewer exposed dogs there. In our model, we assume that susceptible and exposed dogs are vaccinated at the same rate. From Fig. 5a,

b, we see that the change in the number of susceptible dogs near the interface is much larger than that of exposed dogs. Thus, the distribution of vaccinated dogs near the interface follows that of susceptible dogs instead of exposed dogs. From the point of view of game theory, susceptible and vaccinated dogs “escape” from the city side to the wild side since there are much fewer infectious dogs on the wild side of the interface and hence the risk of being infected is much smaller there. Thus, these “ridges” and “valleys” near the interface for different dog compartments can be regarded as a strategy of dogs in getting rid of rabies. This phenomenon is similar to that in Fig. 22b of Potapov et al. (2014) where individuals concentrate in the domain of smaller diffusion rate near the interface, though the diffusion rate is discontinuous at the interface between “good” and “bad” habitats in Potapov et al. (2014).

For the cases with heterogeneous initial conditions, wherever the initial infections are located, the disease always spreads out to the rabies-free areas and eventually distributes throughout the entire spatial domain (see supplementary Figs. 20, 21 and 22 in Appendix). The population waves of susceptible, exposed, infectious, and vaccinated dogs all progress faster in the wild region than in the city region (see Figs. 6, 7 and 8). A comparison of epizootic progression with the four different initial conditions is given in Fig. 9. In all these four cases, a much smaller peak follows the first outbreak. The speed of the epizootic waves changes when they pass through the interface between city and wild regions. This is like the transmission of sound from one medium into another where the speed also changes.

### 5.3 Rabies Control by Vaccination

Different landscapes require different vaccination distribution methods. In the city region, since most dogs are domestic, the commonly used method to deliver vaccination is via injection. In the wild region, vaccines are usually distributed via baits dropped from helicopters or aircrafts. However, this method is not recommended in the city region since the baits may be picked up by children although they are not dangerous. Cost-effectiveness also needs to be considered in deciding when, where, and how to deliver the vaccines. In this section, we explore the effects of three different vaccination strategies (homogeneous, city-focused, and wild-focused) for rabies control in the scenario of city-wild diffusion and homogeneous initial condition. One of the results of interest is whether it is possible to control rabies by vaccinating dogs purely in the city region or in the wild region.

In Fig. 10, a larger vaccination rate leads to a smaller infectious dog population size at the steady state. The “up and down” near the interface between city and wild regions exists for all levels of vaccination strengths but are obviously weakened when the vaccination rate is very large.

We use the function  $k(x) = \alpha(-0.0327 \arctan(x - 50) + 0.051)$  to describe city-focused vaccination rate. This transformation of the arctan function satisfies the expected qualitative behavior of the vaccination rate with positive values in city region and near zero in wild region. A greater value of  $\alpha$  corresponds to a larger vaccination rate in the city region (see Fig. 11a). As can be seen from Fig. 11b, a stronger city-focused vaccination rate can reduce the number of infectious dogs at the steady state

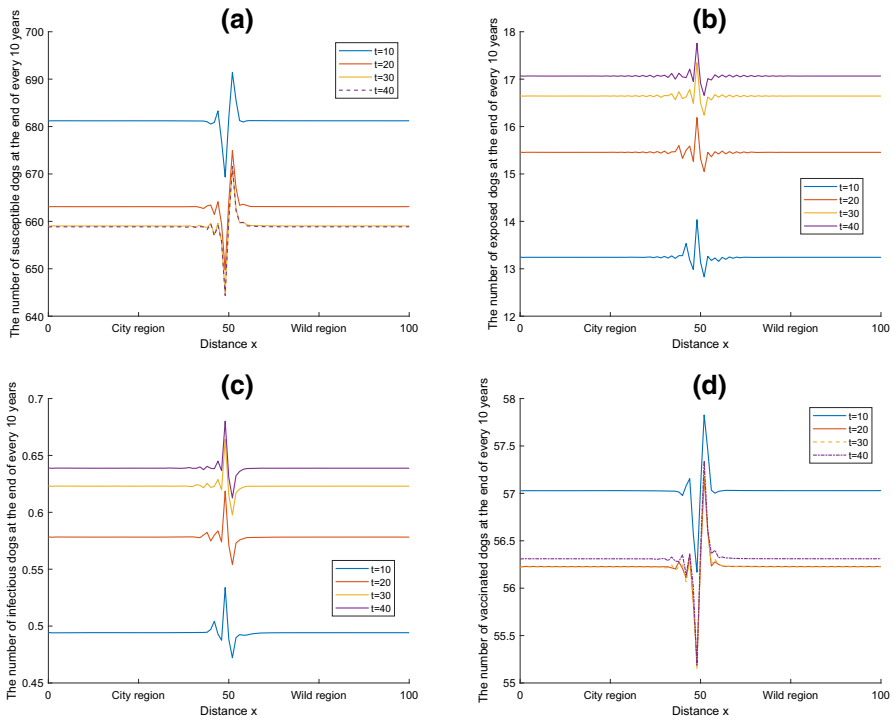


**Fig. 5** The number of susceptible, exposed, infectious, and vaccinated dogs at the end of every 10 years with homogeneous initial condition given in Sect. 5.1.1.  $D_I(x) = \frac{13}{6} \arctan(x - 50) + \frac{15}{4}$ ,  $k = 0.09$ , and the other parameter values are the same as those in Table 1

to a lower level in the city region but city-focused vaccination almost has no effect on the steady state of infectious dogs in the internal wild region. Thus, it is impossible to eliminate rabies in the entire domain by increasing the vaccination rate in the city region only. In addition, from supplementary Fig. 23 we find that a strong city-focused vaccination can put off the outbreak of rabies in the city region, however, it has no effect on the epizootics in the wild region. Traveling waves or epizootic waves are observed in the city region when the vaccination rate is about 0.6 or 0.7 (i.e.,  $\alpha = 6$  or 7) in the city region (see supplementary Figs. 23g, h). When the vaccination rate is about 0.8 (i.e.,  $\alpha = 8$ ) in the city region, there is no disease outbreak in the city region; however, several outbreaks still occur in the wild region (see supplementary Fig. 23i).

Another vaccination strategy is wild-focused. Figure 12a shows the wild-focused vaccination rates obtained by reversing the city-focused vaccination rate with respect to the interface  $x = 50$ . The effects of different wild-focused vaccination rates are shown in Fig. 12b. We see that a greater wild-focused vaccination rate can reduce the number of infectious dogs at the steady state in the wild region. However, no matter how strong the wild-focused vaccination is, the number of infectious dogs in the city region almost remains unchanged at a high level. This indicates that it is impossible

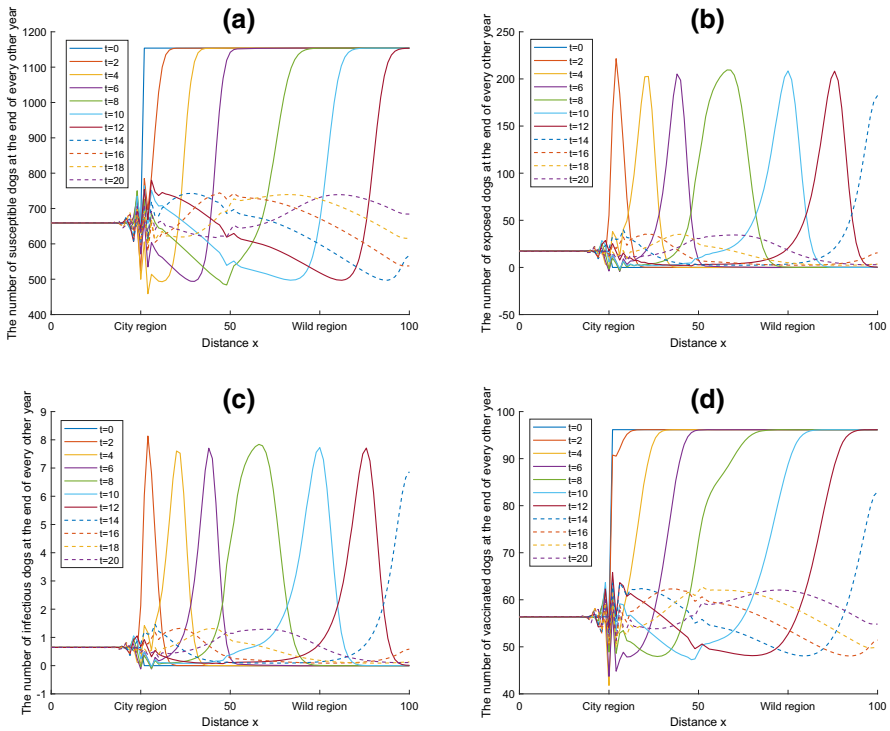
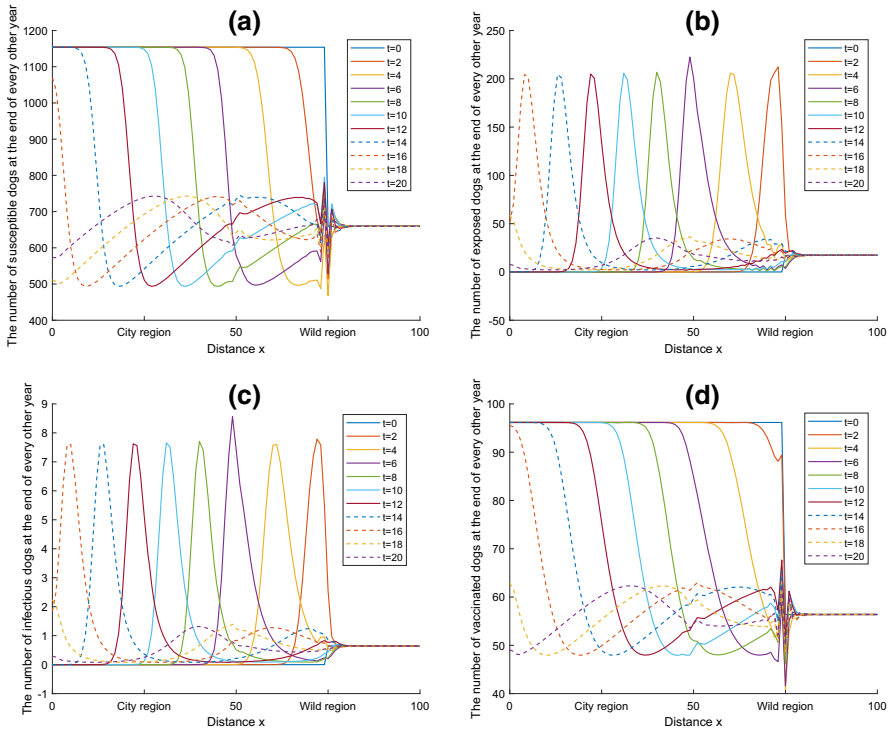


**Fig. 6** The number of susceptible, exposed, infectious, and vaccinated dogs at the end of every other year with initial infections in the city region as given in Sect. 5.1.2.  $D_I(x) = \frac{13}{6} \arctan(x - 50) + \frac{15}{4}$ ,  $k = 0.09$ , and the other parameter values are the same as those in Table 1

to eliminate rabies in the entire domain if the vaccination is purely focused in the wild region. The long-term spatial distributions of infectious dogs under different wild-focused vaccination rates are given in supplementary Fig. 24. The results in Fig. 24 are almost symmetric to those in Fig. 23 with respect to the interface between city and wild regions.

### 6 Gaussian-Type Diffusion

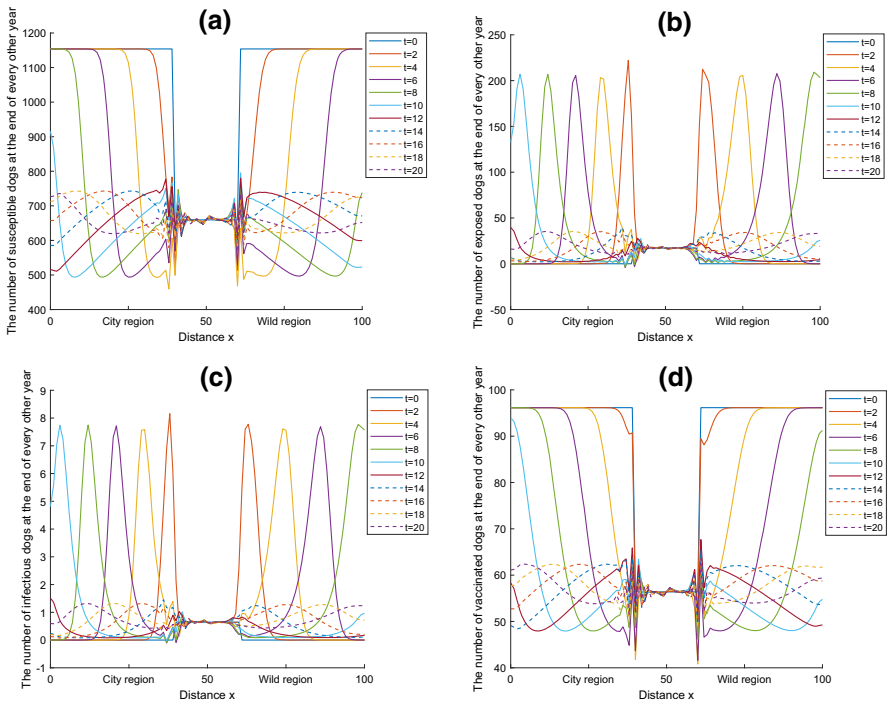
The diffusion rate of dogs typically varies with the class of landscapes. For instance, within one city, dogs usually have larger diffusion rates in the outdoor open region and smaller diffusion rates in the block region. In wild regions, dogs in different landscapes, such as grassland, forest, and wetland, can also have different diffusion rates. In this section, we investigate rabies transmission dynamics when the diffusion rate of infectious dogs in model (3) is a combination of Gaussian functions. This Gaussian-type diffusion is a prototype of many common diffusions in spatially heterogeneous environments.



**Fig. 7** The number of susceptible, exposed, infectious, and vaccinated dogs at the end of every other year with initial infections in the wild region as given in Sect. 5.1.3.  $D_I(x) = \frac{13}{6} \arctan(x - 50) + \frac{15}{4}$ ,  $k = 0.09$ , and the other parameter values are the same as those in Table 1

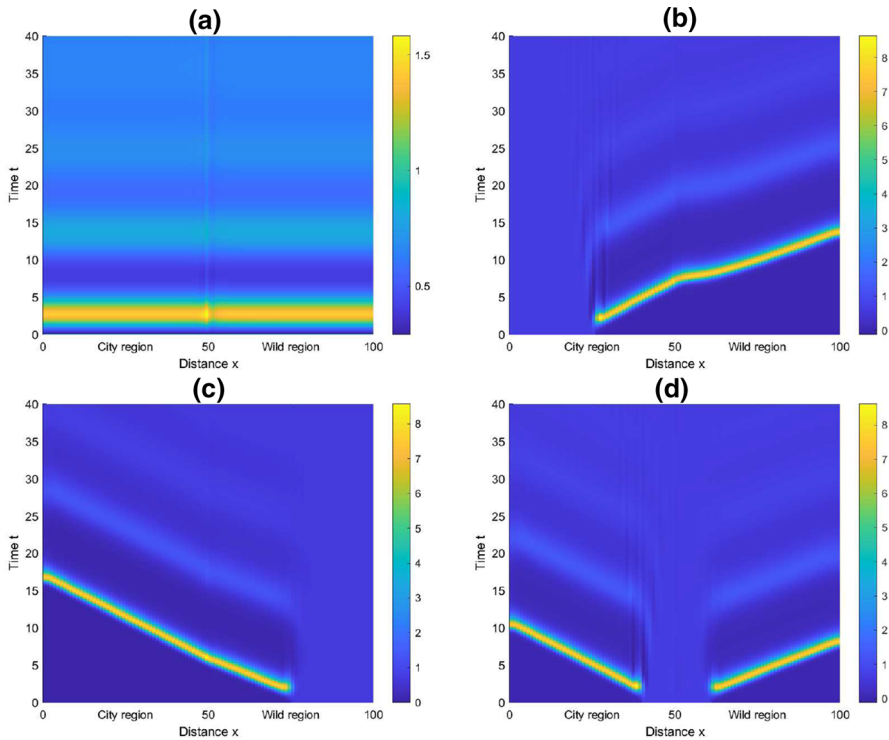
The steady states of infectious dogs with Gaussian diffusion under two different initial conditions are given in Fig. 13. The diffusion rate is a combination of two Gaussian functions, and its curve has two peaks (see the blue curves in Fig. 13). A local maximum of the diffusion rate corresponds to a local minimum of the steady-state distribution of infectious dogs. A larger local maximum of the diffusion rate will pull the population of infectious dogs to a lower level at the corresponding location. Besides, we see that different initial conditions have little impact on the steady state distribution. In general, if the diffusion rate is large at a location, then the population of infectious dogs at the steady state is small at that location. This seems intuitively reasonable since the infectious dogs with a larger diffusion rate tend to disperse far away so that their population becomes smaller at the original location and hence the risk of being bitten by infectious dogs also decreases for the susceptible dogs at that location leading to fewer infected dogs there. Once the infectious dogs arrive at a location that renders an extremely small diffusion rate, it is less possible for them to disperse far away so that the chance of coming into contact with the susceptible dogs at that location increases resulting in more infected dogs there.

Figure 14 compares the long-term spatial distributions of infectious dogs with Gaussian diffusion under homogeneous initial condition and stepwise initial condition. For



**Fig. 8** The number of susceptible, exposed, infectious, and vaccinated dogs at the end of every other year with initial infections around the interface between city and wild regions as given in Sect. 5.1.4.  $D_I(x) = \frac{13}{6} \arctan(x - 50) + \frac{15}{4}$ ,  $k = 0.09$ , and the other parameter values are the same as those in Table 1

both cases, the first outbreak is followed by a second outbreak with much smaller peaks and then followed by a third outbreak with further smaller peaks. “Sinks” appear in the infectious dog distribution corresponding to the peak values of the diffusion rate. With the stepwise initial condition, the disease spreads to disease-free area and eventually distribute throughout the entire spatial domain. Epizootic waves are observed under stepwise initial condition but not with homogeneous initial condition. The progression speed of the waves slightly slows down when the wave peak arrives at the location corresponding to the local maximum of the Gaussian diffusion rate (see Fig. 14). Figure 15 gives the distribution of susceptible, exposed, infectious and vaccinated dogs at the end of every other year, which makes the observation of epizootic waves clearer. For the long-term dynamics of dogs in all the four compartments with Gaussian diffusion under the two different initial conditions, see supplementary Figs. 25 and 26 . The average steady-state distributions of dogs with the Gaussian diffusion are similar to those with homogeneous diffusion in Sect. 4 except some wavy ups and downs induced by the Gaussian-type diffusion.



**Fig. 9** 2-D view of long-term spatial distributions of infectious dogs with city-wild diffusion and four different initial conditions: **a** homogeneous initial condition as given in Sect. 5.1.1; **b** initial infections in the city region as given in Sect. 5.1.2; **c** initial infections in the wild regions as given in Sect. 5.1.3; **d** initial infections around the interface between city and wild regions as given in Sect. 5.1.4.  $D_I(x) = \frac{13}{6} \arctan(x - 50) + \frac{15}{4}$ ,  $k = 0.09$ , and the other parameter values are the same as those in Table 1

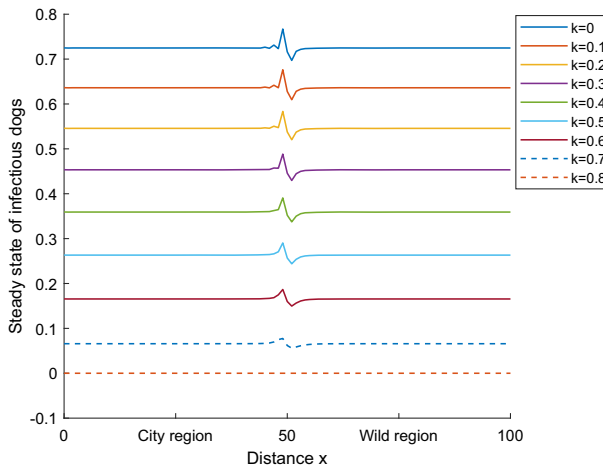


**Fig. 10** The steady states of infectious dogs under different homogeneous vaccination rates.  $D_I(x) = \frac{13}{6} \arctan(x - 50) + \frac{15}{4}$ , and the other parameter values are the same as those in Table 1

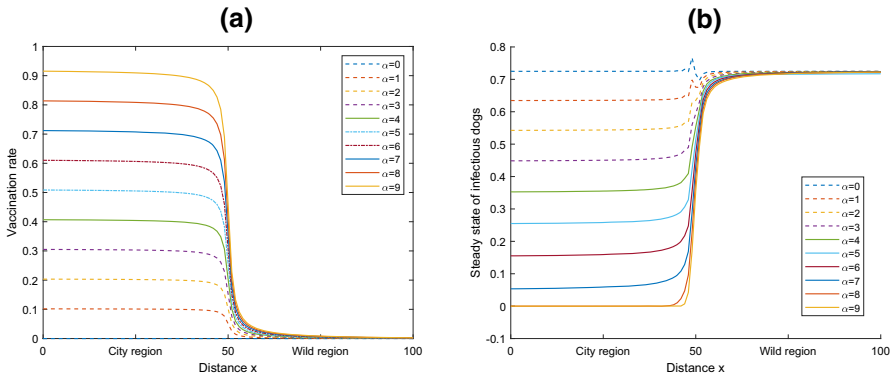


**Fig. 11** **a** City-focused vaccination rate  $k(x) = \alpha(-0.0327 \arctan(x - 50) + 0.051)$ ; **b** steady states of infectious dogs under different city-focused vaccination rates  $k(x) = \alpha(-0.0327 \arctan(x - 50) + 0.051)$  where  $\alpha = 0, 1, 2, 3, 4, 5, 6, 7, 8, 9$ .  $D_I(x) = \frac{13}{6} \arctan(x - 50) + \frac{15}{4}$ , and the other parameter values are the same as those in Table 1. The initial condition is  $S(x, 0) = 800, E(x, 0) = 5, I(x, 0) = 2, R(x, 0) = 10$

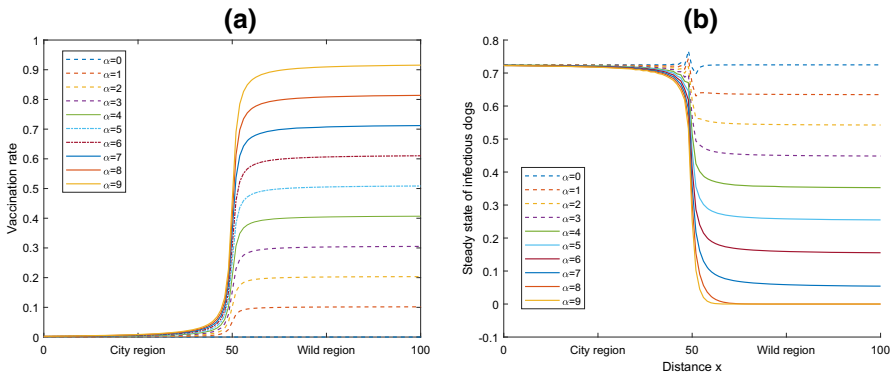


**Fig. 12** **a** Wild-focused vaccination rate  $k(x) = \alpha(0.0327 \arctan(x - 50) + 0.051)$ ; **b** steady states of infectious dogs under different wild-focused vaccination rates  $k(x) = \alpha(0.0327 \arctan(x - 50) + 0.051)$  where  $\alpha = 0, 1, 2, 3, 4, 5, 6, 7, 8, 9$ .  $D_I(x) = \frac{13}{6} \arctan(x - 50) + \frac{15}{4}$ , and the other parameter values are the same as those in Table 1. The initial condition is  $S(x, 0) = 800, E(x, 0) = 5, I(x, 0) = 2, R(x, 0) = 10$

### 7 Incorporation of Seasonal Transmission

Seasonal mechanisms can be of great importance in determining rabies virus maintenance in domestic and wildlife systems (see, e.g., George et al. 2011; Ruan 2017a). Thus, it is reasonable that some parameters vary seasonally. For instance, the biting rate could be higher in warm seasons and lower in cold seasons since it is strongly associated with the activities of dogs. In this section, we present the preliminary result for a seasonal transmission model and set the stage for future research of rabies transmission with seasonality. Based on model (3), we assume that the biting rate  $\beta(t) = 0.25 \times (1 + 0.41 \sin(2\pi t + 5.5))$ , as given by the function in Fig. 16a, which is positive, continuous and periodic due to seasonality. We also assume that the diffusion

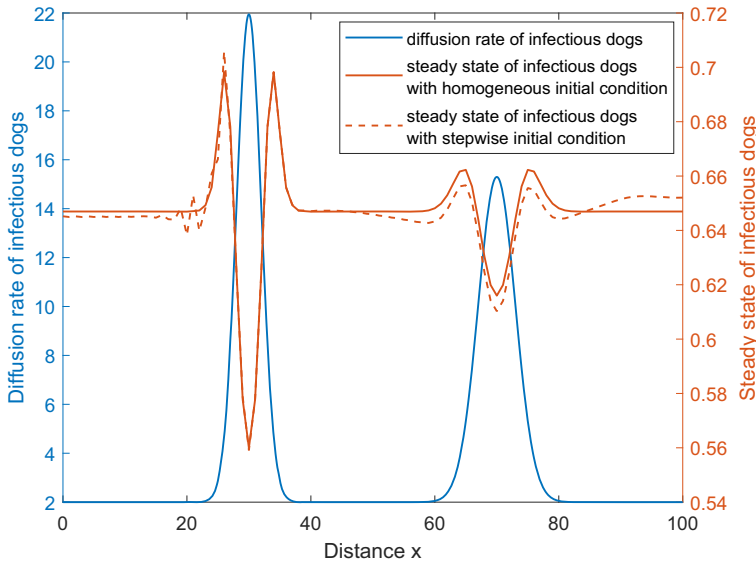


**Fig. 13** Blue curve: diffusion rate of infectious dogs; red solid curve: steady state of infectious dogs with homogeneous initial condition given in Sect. 4.1.1; red dash curve: steady state of infectious dogs with stepwise initial condition given in Sect. 4.1.2.  $D_I(x) = 2 + \frac{50}{\sqrt{2\pi}} \exp\left(-\frac{(x-30)^2}{8}\right) + \frac{100}{3\sqrt{2\pi}} \exp\left(-\frac{(x-70)^2}{18}\right)$ ,  $k = 0.09$ , and the other parameter values are the same as those in Table 1

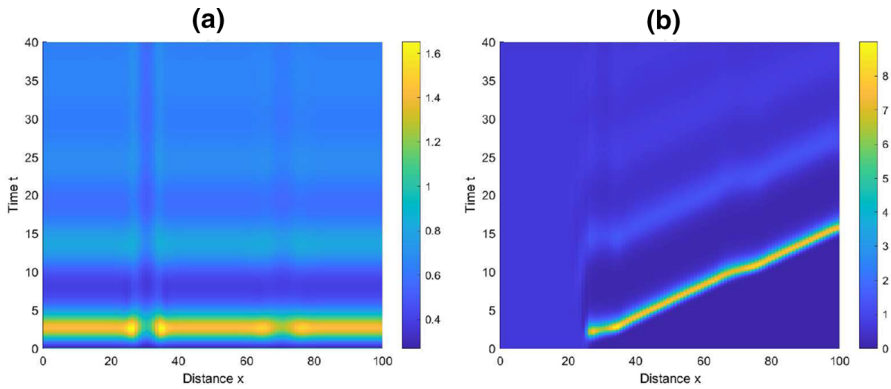


**Fig. 14** 2-D view of long-term spatial distributions of infectious dogs with Gaussian-type diffusion under different initial conditions: **a** homogeneous initial condition given in Sect. 4.1.1; **b** stepwise initial condition given in Sect. 4.1.2.  $D_I(x) = 2 + \frac{50}{\sqrt{2\pi}} \exp\left(-\frac{(x-30)^2}{8}\right) + \frac{100}{3\sqrt{2\pi}} \exp\left(-\frac{(x-70)^2}{18}\right)$ ,  $k = 0.09$ , and the other parameter values are the same as those in Table 1

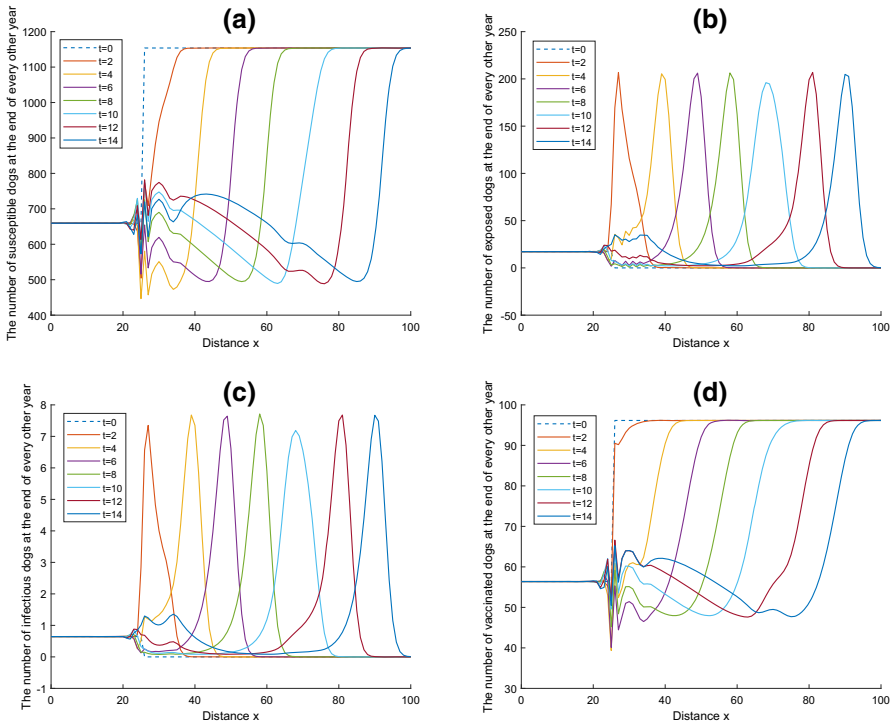


**Fig. 15** The number of susceptible, exposed, infectious, and vaccinated dogs at the end of every other year with stepwise initial condition given in Sect. 4.1.2.  $D_I(x) = 2 + \frac{50}{\sqrt{2\pi}} \exp\left(-\frac{(x-30)^2}{8}\right) + \frac{100}{3\sqrt{2\pi}} \exp\left(-\frac{(x-70)^2}{18}\right)$ ,  $k = 0.09$ , and the other parameter values are the same as those in Table 1

is over a city-wild landscape with  $D_I(x) = \frac{13}{6} \arctan(x - 50) + \frac{15}{4}$ . Then, we have the following time-periodic partial differential equation model.

$$\begin{aligned}
 \frac{\partial S(x, t)}{\partial t} &= a + \lambda R(x, t) + \sigma(1 - \gamma)E(x, t) - \beta(t)S(x, t)I(x, t) - (m + k)S(x, t), \\
 \frac{\partial E(x, t)}{\partial t} &= \beta(t)S(x, t)I(x, t) - \sigma E(x, t) - (m + k)E(x, t), \\
 \frac{\partial I(x, t)}{\partial t} &= \sigma \gamma E(x, t) - (m + \mu)I(x, t) + \frac{\partial^2}{\partial x^2}(D_I(x)I(x, t)), \\
 \frac{\partial R(x, t)}{\partial t} &= k(S(x, t) + E(x, t)) - (m + \lambda)R(x, t),
 \end{aligned}
 \tag{6}$$

with homogeneous Neumann boundary condition.

Figure 16b shows that the infectious dog population fluctuates periodically, even during an epidemic outbreak. The periodic dynamics for all the four compartments between the 30th and 40th years are given in Fig. 27 in Appendix. The interface

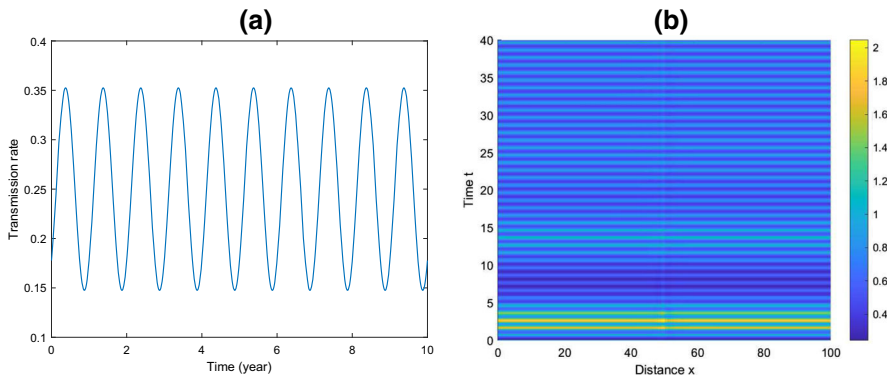


**Fig. 16** **a** Seasonal biting rate  $\beta(t) = 0.25 \times (1 + 0.41 \sin(2\pi t + 5.5))$ ; **b** 2-D view of the seasonal fluctuation of infectious dog population in city-wild landscape.  $D_I(x) = \frac{13}{6} \arctan(x - 50) + \frac{15}{4}$ ,  $k = 0.09$ , and the other parameter values are the same as those in Table 1. The initial condition is  $S(x, 0) = 800$ ,  $E(x, 0) = 5$ ,  $I(x, 0) = 1$ ,  $R(x, 0) = 10$

between city and wild regions remain “active” as the autonomous case and are more obvious to observe for the susceptible and vaccinated populations.

## 8 Discussion

In this paper, we developed a dog rabies model in which the diffusion of dog population is described by the  $\theta$ -diffusion term. The parameter  $\theta$  corresponds to the way each individual dog makes movement decisions in the underlying random walk. The movements of infectious and non-infectious dogs are essentially different. Infectious dogs move randomly due to their destroyed central nervous systems, whereas non-infectious dogs can make movement decisions based on the conditions at specific locations. We focused on the model with the diffusion of only infectious dogs since in most cases the diffusion of non-infectious dogs can be negligible compared with the much higher diffusion rate of infectious dogs. We numerically investigated rabies transmission dynamics in three cases: (i) a spatially homogeneous environment; (ii) city and wild regions; (iii) various landscapes. The difference among these three cases is reflected in the diffusion rate of infectious dogs in the model. The homogeneous environment leads to a constant diffusion rate. The city-wild case gives rise to a diffusion rate function which has smaller values in the city region and larger values in the wild region. Given a mixture of various landscapes, the diffusion rate can be described by a combination of Gaussian functions. For all these three cases, traveling waves or epizootic waves are observed when the initial condition is of stepwise type in which the initial infectious dogs are concentrated in a subregion of the entire spatial domain. The speed of the epizootic waves changes when they progress through the interface between two different environments. However, the steady state of dog population is little affected by the initial conditions. An “up and down” is observed near the interface between city and wild regions: the exposed and infectious dog population sizes bounce to form a “ridge” on the city side; the susceptible and vaccinated fall below the

average level on the city side and a “valley” occurs. The city-wild scenario is closely related to public health. We examined three different vaccination strategies for dogs in city and wild regions: (i) homogeneous vaccination; (ii) city-focused vaccination; (iii) wild-focused vaccination. We found that for some specific city-focused and wild-focused vaccination rates, traveling waves or epizootic waves can occur even if the initial condition is homogeneous, which would be impossible if the vaccination rate is homogeneous. Although a high city-focused vaccination rate can well control rabies in the city region, it is impossible to eliminate rabies in both city and wild regions if the vaccination is focused in the city region only, similar with the case of wild-focused vaccination. The steady state of infectious dogs under a Gaussian-type diffusion shows that a local maximum of the Gaussian-type diffusion rate corresponds to a local minimum of the steady state, which indicates that a strong diffusion of infectious dogs at a location weakens the epizootic scale there. When the biting rate is seasonally varying, the dog population size approaches a positive time-periodic spatially heterogeneous distribution eventually.

The  $\theta$ -diffusion equation has many applications in the study of ecological problems such as finding the evolutionarily stable strategy. To our knowledge this paper is the first one that applies the general  $\theta$ -diffusion equation to infectious disease modeling. In particular, none of the existing rabies models have used the term  $(D_I(x)I(x, t))_{xx}$ , where  $D_I(x)$  is spatially dependent, to describe the diffusion of infectious dogs. This Fokker–Planck dispersal term not only reflects the random movement of infectious dogs but also accommodates spatial heterogeneity. Although several recent works have investigated the basic reproduction number for PDE systems with Fickian diffusion, there has been no practical method that can be used to calculate the basic reproduction number for PDE systems with Fokker–Planck diffusion. It would be an important work to derive the basic reproduction number for PDE systems with non-standard diffusion terms. It is also interesting to investigate the dynamics of model (2) with more spatially dependent parameters and to explore how the basic reproduction number depends on the movement decisions of non-infectious dogs. We leave these for future investigation.

For the numerical simulations in this paper, we focused on one-dimensional space and used the same parameter values as most of those in Zhang et al. (2012). Future simulations are expected based on satellite tracking data about dog or other wildlife populations in two-dimensional spatial domains so as to predict the emergence and spread of rabies in a specific region. Furthermore, we can use the optimal control theory or cost-effectiveness analysis to best allocate public health resources such as vaccines in controlling rabies. The incubation period of rabies infections can be described in terms of a time delay instead of the exposed compartment. In that case, a delay reaction–diffusion equation arises. It is interesting to compare the simulation results of such a delay equation with the ones in this paper. We also hope that our work can motivate some qualitative analysis of partial differential equation models with non-standard diffusion terms.

**Acknowledgements** We are very thankful to the two anonymous referees for their insightful comments and helpful suggestions that greatly improved our manuscript.

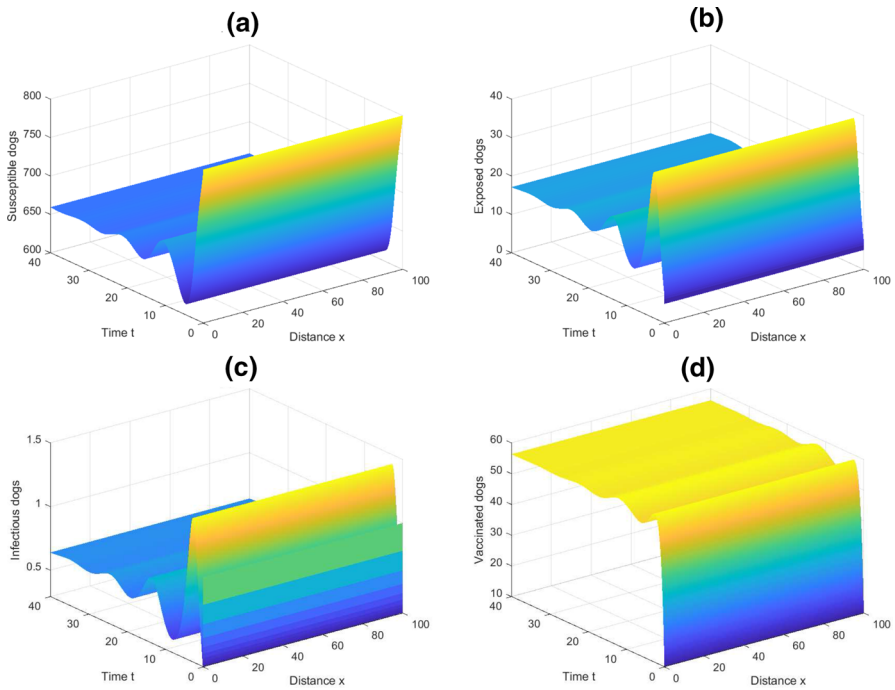


**Fig. 17** Long-term spatial distribution of susceptible, exposed, infectious, and vaccinated dogs with homogeneous initial condition given in Sect. 4.1.1.  $D_I(x) = 5$ ,  $k = 0.09$ , and other parameter values are the same as those in Table 1

## Appendix: supplementary figures

In this Appendix, we provide supplementary figures. For the homogeneous diffusion in Sect. 4, the spatiotemporal dynamics of dogs under the homogeneous initial condition and the stepwise initial condition are given in Figs. 17 and 18, respectively. For the city-wild diffusion in Sect. 5, Fig. 19 gives the long-term spatial dynamics of dogs under the homogeneous initial condition. Figures 20, 21, and 22 give the long-term spatial dynamics of dogs under the initial conditions with infections in city region, in wild region, and around the city-wild interface, respectively. Figure 23 compares nine different strengths of city-focused vaccinations, and Fig. 24 compares nine different strengths of wild-focused vaccinations. For the Gaussian-type diffusion in Sect. 6, the long-term dynamics of dogs under the homogeneous initial condition and the stepwise initial condition are given in Figs. 25 and 26, respectively. For model (6) with seasonal biting rate and city-wild diffusion, the spatially seasonal dynamics of dogs is given in Figure 27.

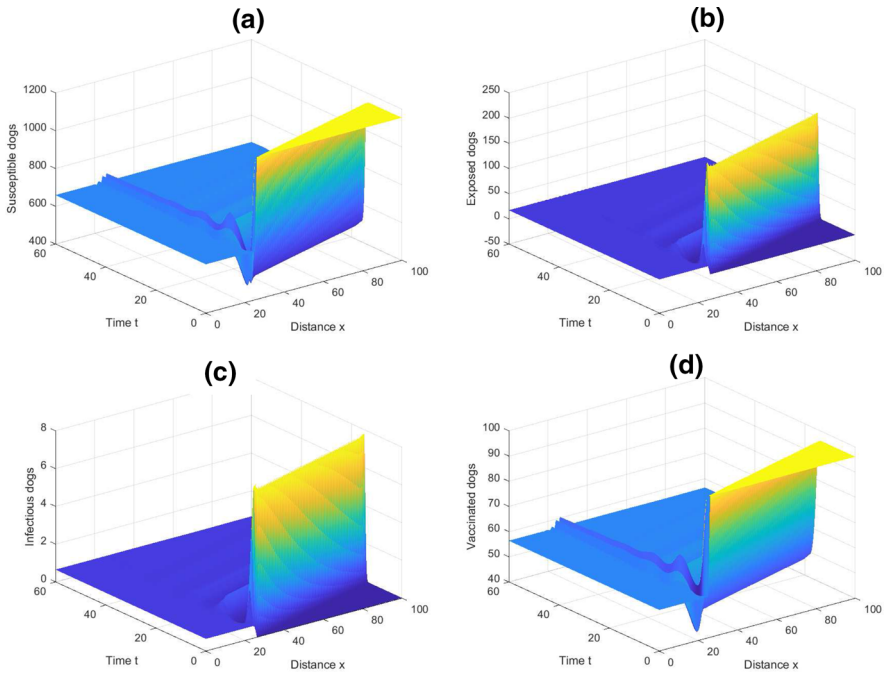


**Fig. 18** Long-term spatial distribution of susceptible, exposed, infectious and vaccinated dogs with stepwise initial condition given in Sect. 4.1.2.  $D_I(x) = 5$ ,  $k = 0.09$ , and the other parameter values are the same as those in Table 1

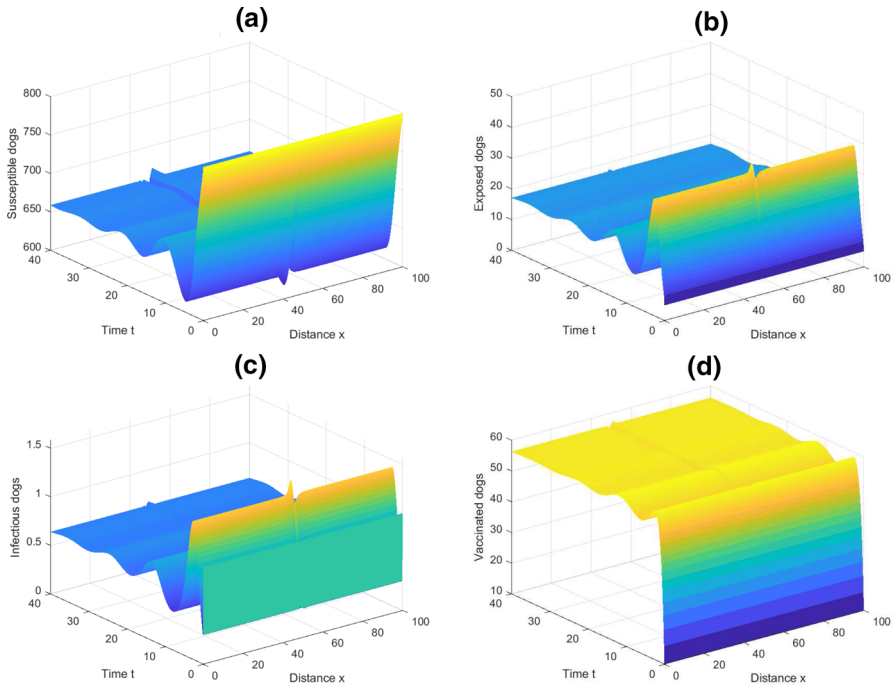


**Fig. 19** Long-term spatial distribution of susceptible, exposed, infectious, and vaccinated dogs with diffusion of infectious dogs in city and wild regions with homogeneous initial condition given in Sect. 5.1.1.  $D_I(x) = \frac{13}{6} \arctan(x - 50) + \frac{15}{4}$ ,  $k = 0.09$ , and the other parameter values are the same as those in Table 1

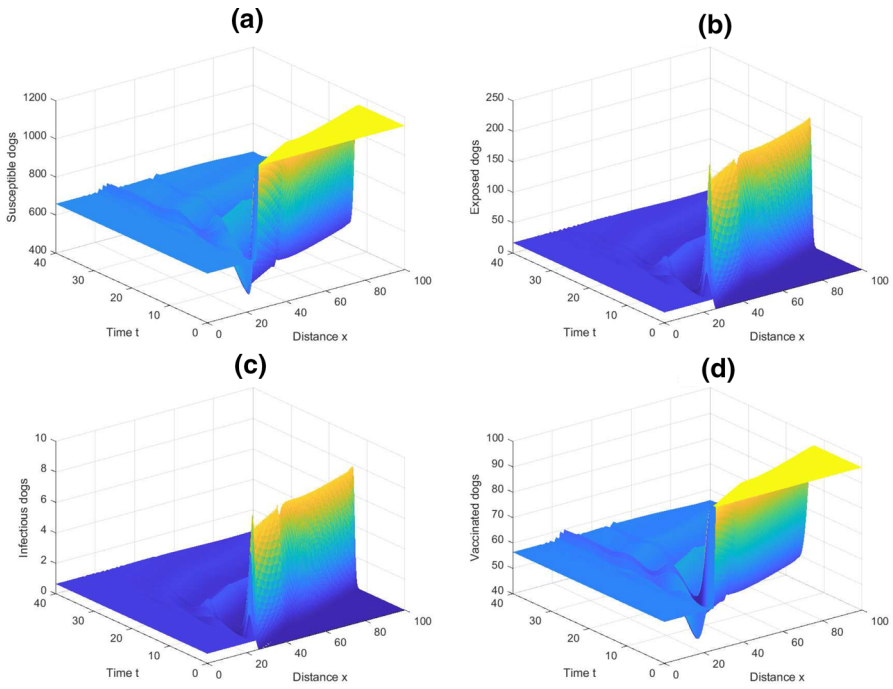


**Fig. 20** Long-term spatial distribution of susceptible, exposed, infectious, and vaccinated dogs with initial infections in the city region given in Sect. 5.1.2.  $D_I(x) = \frac{13}{6} \arctan(x - 50) + \frac{15}{4}$ ,  $k = 0.09$ , and the other parameter values are the same as those in Table 1

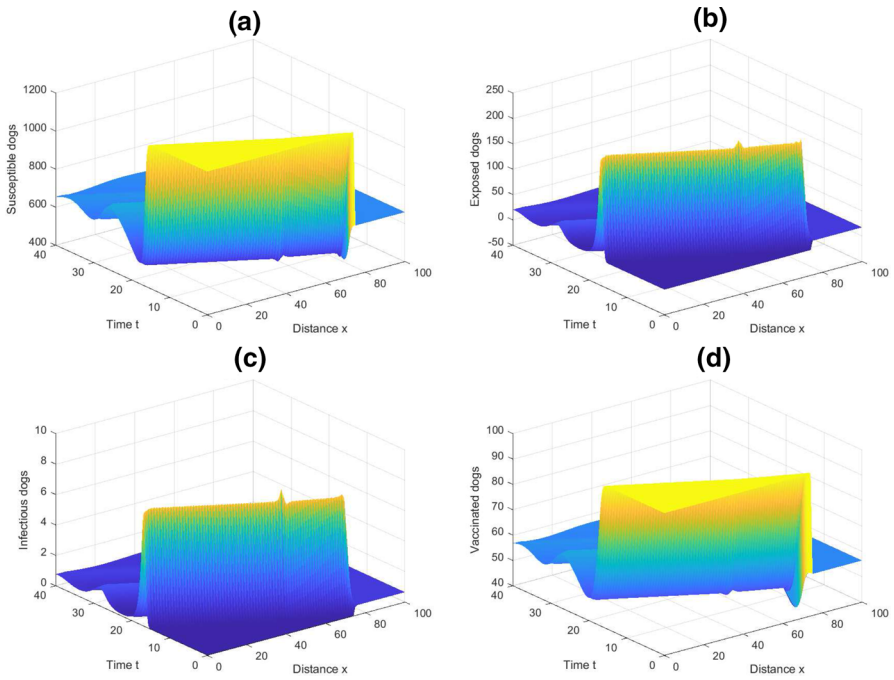


**Fig. 21** Long-term spatial distribution of susceptible, exposed, infectious and vaccinated dogs with initial infections in the wild region given in Sect. 5.1.3.  $D_I(x) = \frac{13}{6} \arctan(x - 50) + \frac{15}{4}$ ,  $k = 0.09$ , and the other parameter values are the same as those in Table 1

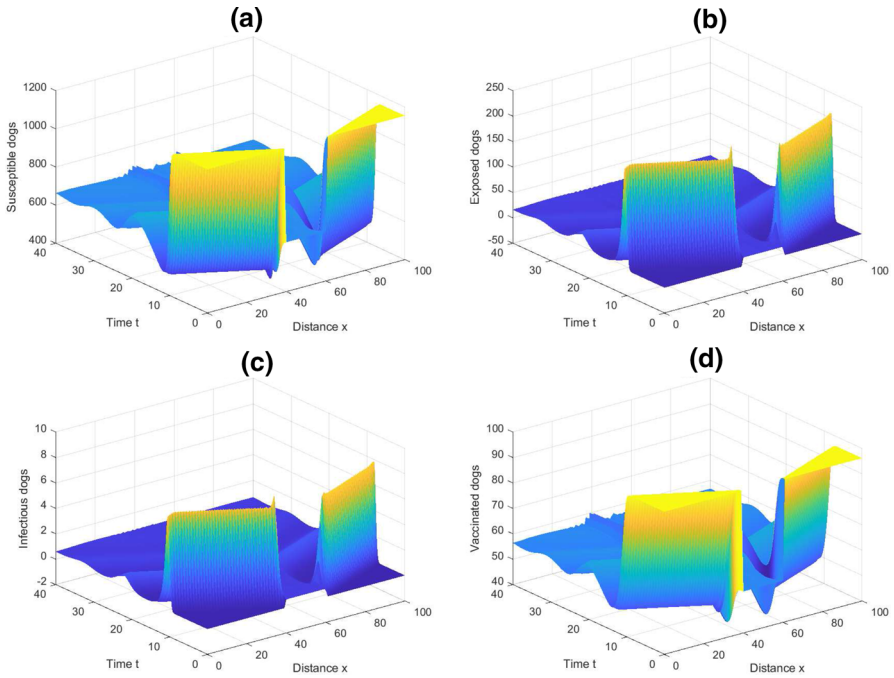


**Fig. 22** Long-term spatial distribution of susceptible, exposed, infectious and vaccinated dogs with initial infections around the interface between city and wild regions given in Sect. 5.1.4.  $D_I(x) = \frac{13}{6} \arctan(x - 50) + \frac{15}{4}$ ,  $k = 0.09$ , and the other parameter values are the same as those in Table 1

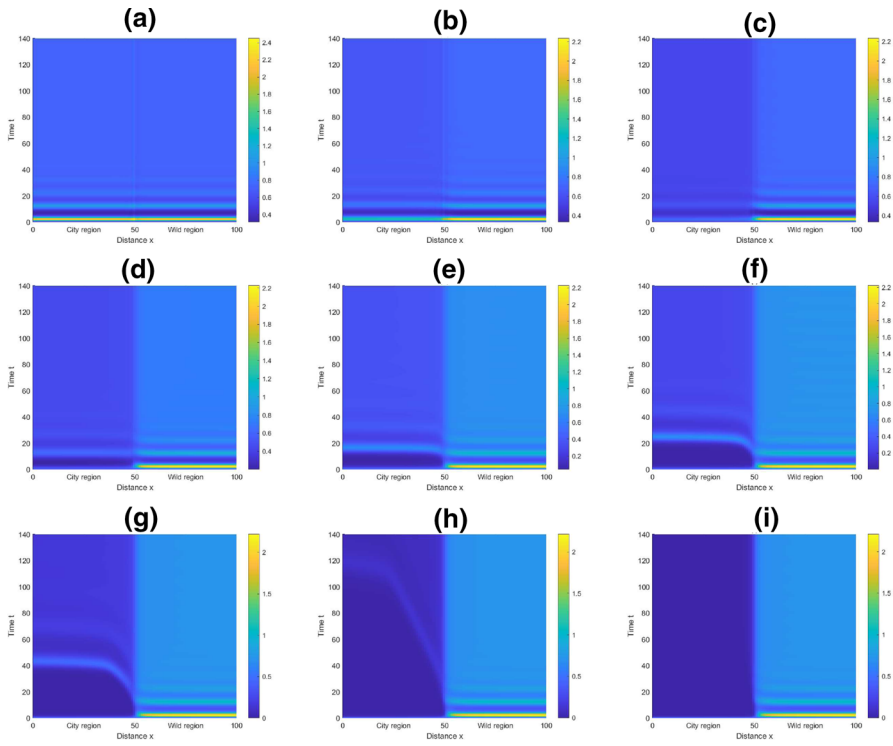


**Fig. 23** Long-term spatial distribution of susceptible, exposed, infectious, and vaccinated dogs with diffusion of infectious dogs in city and wild regions and city-focused vaccination  $k = \alpha(-0.0327 \arctan(x - 50) + 0.051)$ . **a**  $\alpha = 0$ ; **b**  $\alpha = 1$ ; **c**  $\alpha = 2$ ; **d**  $\alpha = 3$ ; **e**  $\alpha = 4$ ; **f**  $\alpha = 5$ ; **g**  $\alpha = 6$ ; **h**  $\alpha = 7$ ; **i**  $\alpha = 8$ .  $D_I(x) = \frac{13}{6} \arctan(x - 50) + \frac{15}{4}$ , and the other parameter values are the same as those in Table 1. The initial condition is  $S(x, 0) = 800$ ,  $E(x, 0) = 5$ ,  $I(x, 0) = 2$ ,  $R(x, 0) = 10$

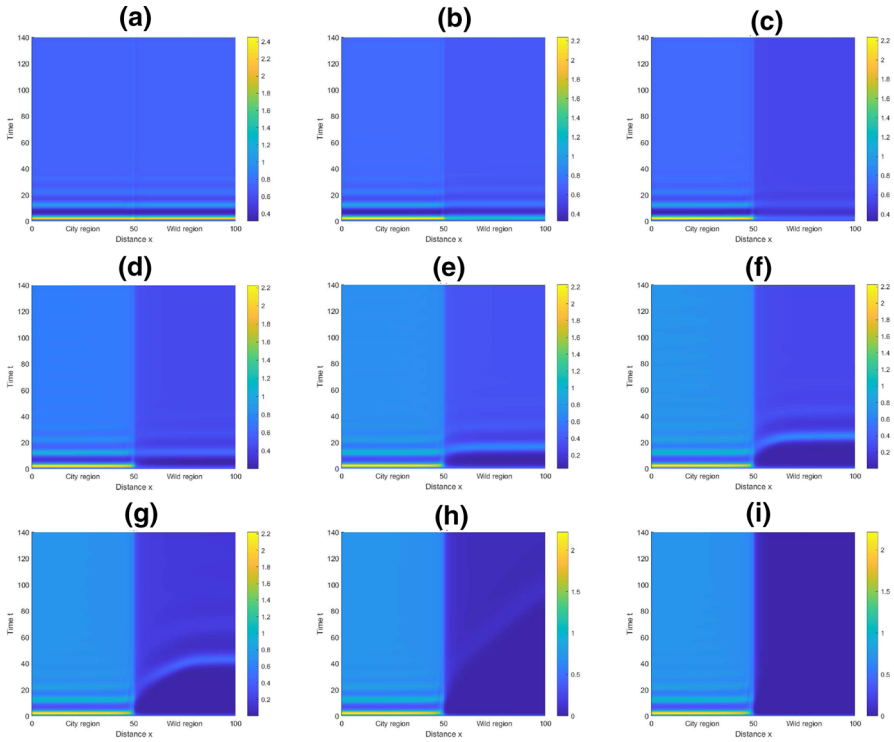


**Fig. 24** Long-term spatial distribution of susceptible, exposed, infectious, and vaccinated dogs with diffusion of infectious dogs in city and wild regions and wild-focused vaccination  $k = \alpha(0.0327 \arctan(x - 50) + 0.051)$ . **a**  $\alpha = 0$ ; **b**  $\alpha = 1$ ; **c**  $\alpha = 2$ ; **d**  $\alpha = 3$ ; **e**  $\alpha = 4$ ; **f**  $\alpha = 5$ ; **g**  $\alpha = 6$ ; **h**  $\alpha = 7$ ; **i**  $\alpha = 8$ .  $D_I(x) = \frac{13}{6} \arctan(x - 50) + \frac{15}{4}$ , and the other parameter values are the same as those in Table 1. The initial condition is  $S(x, 0) = 800$ ,  $E(x, 0) = 5$ ,  $I(x, 0) = 2$ ,  $R(x, 0) = 10$

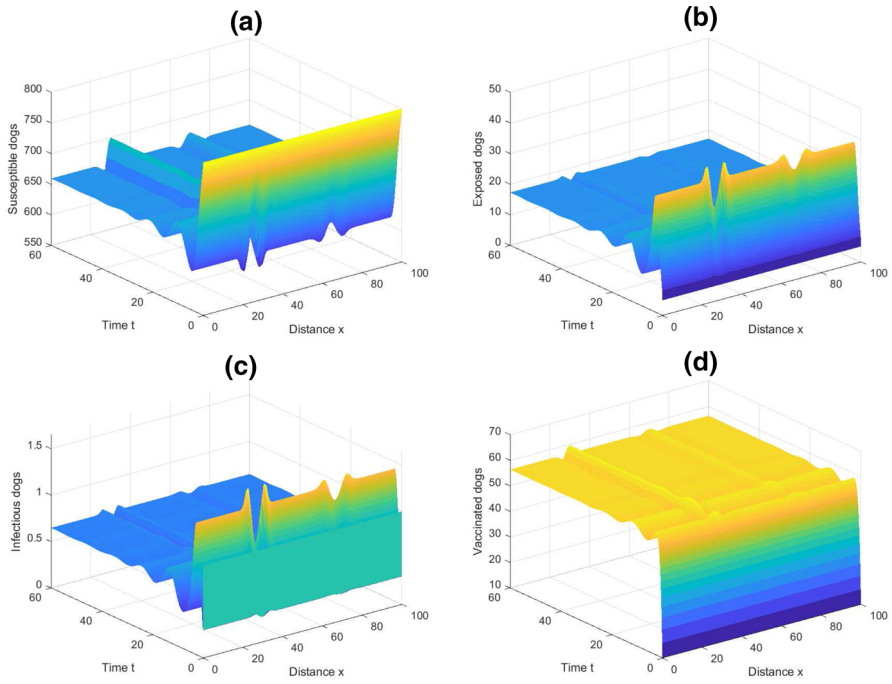


**Fig. 25** Long-term spatial distribution of susceptible, exposed, infectious and vaccinated dogs with homogeneous initial condition given in Sect. 4.1.1.  $D_I(x) = 2 + \frac{50}{\sqrt{2\pi}} \exp\left(-\frac{(x-30)^2}{8}\right) + \frac{100}{3\sqrt{2\pi}} \exp\left(-\frac{(x-70)^2}{18}\right)$ ,  $k = 0.09$ , and the other parameter values are the same as those in Table 1

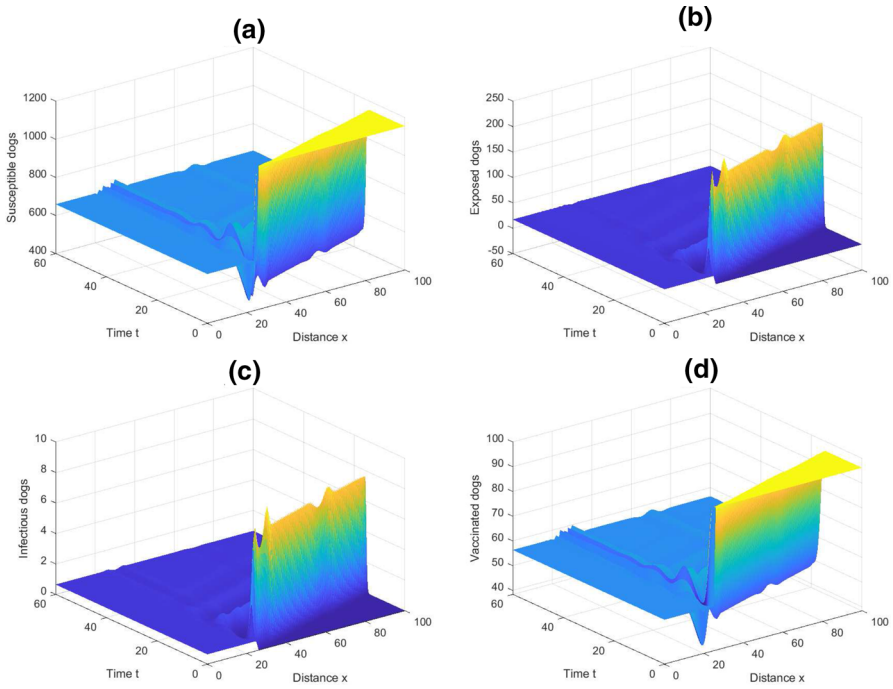


**Fig. 26** Long-term spatial distribution of susceptible, exposed, infectious and vaccinated dogs with stepwise initial condition given in Sect. 4.1.2.  $D_I(x) = 2 + \frac{50}{\sqrt{2\pi}} \exp\left(-\frac{(x-30)^2}{8}\right) + \frac{100}{3\sqrt{2\pi}} \exp\left(-\frac{(x-70)^2}{18}\right)$ ,  $k = 0.09$ , and the other parameter values are the same as those in Table 1

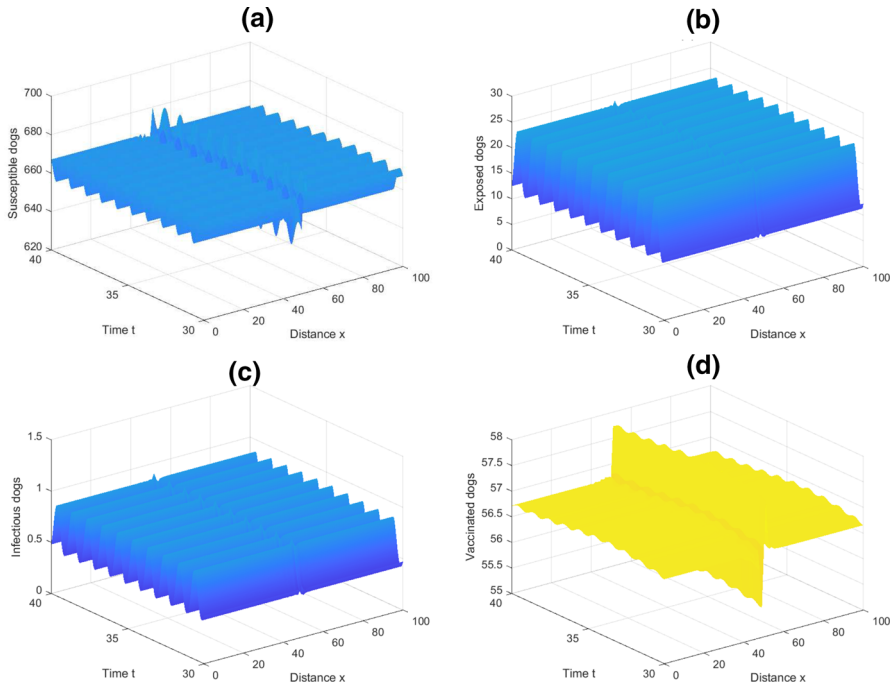


**Fig. 27** Spatial distribution of dogs from the 30th to the 40th year. Here  $\beta(t) = 0.25 \times (1 + 0.41 \sin(2\pi t + 5.5))$ ,  $D_I(x) = \frac{13}{6} \arctan(x - 50) + \frac{15}{4}$ ,  $k = 0.09$ , and the other parameter values are the same as those in Table 1. The initial condition is  $S(x, 0) = 800$ ,  $E(x, 0) = 5$ ,  $I(x, 0) = 1$ ,  $R(x, 0) = 10$

## References

- Allen LJS, Flores DA, Ratnayake RK, Herbold JR (2002) Discrete-time deterministic and stochastic models for the spread of rabies. *Appl Math Comput* 132:271–292
- Anderson RM, Jackson HC, May RM, Smith AM (1981) Population dynamics of fox rabies in Europe. *Nature* 289:765–771
- Benavides JA, Valderrama W, Streicker DG (2016) Spatial expansions and travelling waves of rabies in vampire bats. *Proc R Soc B Biol Sci* 283:20160328
- Borchering RK, Liu H, Steinhaus MC, Gardner CL, Kuang Y (2012) A simple spatiotemporal rabies model for skunk and bat interaction in northeast Texas. *J Theor Biol* 314:16–22
- Center for Disease Control and Prevention (2019) Rabies. <https://www.cdc.gov/rabies>
- Diekmann O, Heesterbeek JAP, Metz AJ (1990) On the definition and the computation of the basic reproduction ratio  $R_0$  in models for infectious diseases in heterogeneous population. *J Math Biol* 28:365–382
- Fofana AM, Hurford A (2017) Mechanistic movement models to understand epizootic spread. *Philos Trans R Soc B* 372:20160086
- George DB, Webb CT, Farnsworth ML, O’Shea TJ, Bowen RA, Smith DL, Stanley TR, Ellison LE, Rupprecht CE (2011) Host and viral ecology determine bat rabies seasonality and maintenance. *PNAS* 108(25):10208–10213
- Hampson K, Dushoff J, Bingham J, Bruckner G, Ali YH, Dobson A (2007) Synchronous cycles of domestic dog rabies in sub-Saharan Africa and the impact of control efforts. *PNAS* 104(18):7717–7722
- Källén A, Arcuri P, Murray JD (1985) A simple model for the spatial spread and control of rabies. *J Theor Biol* 116:377–393
- Kaplan C (1977) Rabies: the facts. Oxford University Press, Oxford
- Liang X, Zhang L, Zhao X-Q (2017) The principal eigenvalue for degenerate periodic reaction-diffusion systems. *SIAM J Math Anal* 49(5):3603–3636
- Macdonald DW (1980) Rabies and wildlife: a biologist’s perspective. Oxford University Press, Oxford
- Magal P, Webb GF, Wu Y (2019) On the basic reproduction number of reaction–diffusion epidemic models. *SIAM J Appl Math* 79(1):284–304
- Mollison D, Kuulasmaa K (1985) Spatial epidemic models: theory and simulations. In: Bacon PJ (ed) Population dynamics of rabies in wildlife. Academic Press, Cambridge, pp 291–309
- Murray JD, Stanley EA, Brown DL (1986) On the spatial spread of rabies among foxes. *Proc R Soc B Biol Sci* 229:111–150
- Neilan RM, Lenhart S (2011) Optimal vaccine distribution in a spatiotemporal epidemic model with an application to rabies and racoons. *J Math Anal Appl* 378:603–619
- Okubo A, Levin SA (2001) Diffusion and ecological problems: modern perspectives. Springer, New York
- Ou C, Wu J (2006) Spatial spread of rabies revisited: influence of age-dependent diffusion on nonlinear dynamics. *SIAM J Appl Math* 67(1):138–164
- Panjeti VG, Real LA (2011) Mathematical models for rabies. *Adv Virus Res* 79:377–395
- Potapov A, Schlögel UE, Lewis MA (2014) Evolutionarily stable diffusive dispersal. *Discrete Contin Dyn B* 19(10):3319–3340
- Rees EE, Pond BA, Tinline RR, Belanger D (2013) Modelling the effect of landscape heterogeneity on the efficacy of vaccination for wildlife infectious disease control. *J Appl Ecol* 50:881–891
- Ruan S (2017) Modeling the transmission dynamics and control of rabies in China. *Math Biosci* 286:65–93
- Ruan S (2017) Spatiotemporal epidemic models for rabies among animals. *Infect Dis Model* 2:277–287
- Smith DL, Lucey B, Waller LA, Childs JE, Real LA (2002) Predicting the spatial dynamics of rabies epidemics on heterogeneous landscapes. *PNAS* 99:3668–3672
- Sterner RT, Smith GC (2006) Modelling wildlife rabies: transmission, economics, and conservation. *Biol Conserv* 131:163–179
- Stuchin M, Machalaba C, Olival KJ, Artois M, Bengis R, Caceres-Soto P, Diaz F, Erlacher-Vindel E, Forcella S, Leighton FA, Murata K, Popovic M, Tizzani P, Torres G, Karesh WB (2018) Rabies as a threat to wildlife. *Rev Sci Tech Off Int Epiz* 37(2):341–357
- Turchin P (1998) Quantitative analysis of movement: measuring and modeling population redistribution of plants and animals. Sinauer Associates, Sunderland
- van den Driessche P, Watmough J (2002) Reproduction numbers and sub-threshold endemic equilibria for compartmental models of disease transmission. *Math Biosci* 180:29–48
- Voigt DR, MacDonald DW (1984) Variation in the spatial and social behavior of the red fox, *Vulpes vulpes*. *Acta Zool Fenn* 171:261–265

- Wang W, Zhao X-Q (2012) Basic reproduction numbers for reaction–diffusion epidemic models. *SIAM J Appl Dyn Syst* 11(4):1652–1673
- World Health Organization (2020) Rabies. <https://www.who.int/health-topics/rabies>
- Zhang J, Jin Z, Sun G, Sun X, Ruan S (2012) Spatial spread of rabies in China. *J Appl Anal Comput* 2(1):111–126
- Zinsstag J, Durr S, Penny MA, Mindekem R, Roth F, Menendez Gonzalez S, Naissengar S, Hattendorf J (2009) Transmission dynamics and economics of rabies control in dogs and humans in an African city. *PNAS* 106(35):14996–5001

**Publisher's Note** Springer Nature remains neutral with regard to jurisdictional claims in published maps and institutional affiliations.